CIRRELT

Centre interuniversitaire de recherche sur les réseaux d'entreprise, la logistique et le transport

Interuniversity Research Centre on Enterprise Networks, Logistics and Transportation

Charge Scheduling for Electric Freight Vehicles

Samuel Pelletier
Ola Jabali
Gilbert Laporte

July 2017

CIRRELT-2017-37

Bureaux de Montréal :
Université de Montréal
Pavillon André-Aisenstadt
C.P. 6128, succursale Centre-ville
Montréal (Québec)
Canada H3C 3J7
Téléphone : 514 343-7575
Télécopie : 514 343-7121

Bureaux de Québec :
Université Laval
Pavillon Palasis-Prince
2325, de la Terrasse, bureau 2642
Québec (Québec)
Canada G1V 0A6
Téléphone : 418 656-2073
Télécopie : 418 656-2624

www.cirrelt.ca

Université Laval · McGill · Université Concordia · ÉTS · UQÀM · HEC Montréal · Polytechnique Montréal · Université de Montréal

Charge Scheduling for Electric Freight Vehicles

Samuel Pelletier[1,*], Ola Jabali[2], Gilbert Laporte[1]

[1] Interuniversity Research Centre on Enterprise Networks, Logistics and Transportation (CIRRELT) and Department of Management Sciences, HEC Montréal, 3000 Côte-Sainte-Catherine, Montréal, Canada H3T 2A7

[2] Dipartimento di Elettronica, Informazione e Bioingegneria, Politecnico di Milano, Piazza Leonardo da Vinci, 32, Milano 20133, Italy

Abstract. We consider a freet of electric freight vehicles that must deliver goods to a set of customers over the course of multiple days. Electric freight vehicles are typically charged at a central depot and rarely use public charging stations during delivery routes. The charging schedule at the depot must be planned ahead of time so as to ensure chargers are available when required and thus allow the vehicles to complete their routes at minimal cost. In addition, high vehicle utilization rates can accelerate battery aging, thereby requiring degradation mitigation considerations. Several numerical experiments are conducted in order to draw managerial insights regarding the impact of battery degradation, grid restrictions, facilities related demand charges, and charger related costs on the charging schedules of electric freight vehicles.

Keywords: Electric vehicles, battery modeling, green transportation, battery degradation, urban logistics.

Acknowledgements. This research was partly supported by the Natural Sciences and Engineering Research Council of Canada (NSERC) under grants 463834-2014, 436014-2013 and 2015-06189. This support is gratefully acknowledged.

Results and views expressed in this publication are the sole responsibility of the authors and do not necessarily reflect those of CIRRELT.

Les résultats et opinions contenus dans cette publication ne reflètent pas nécessairement la position du CIRRELT et n'engagent pas sa responsabilité.

---

* Corresponding author: Samuel.Pelletier@cirrelt.ca

Dépôt légal – Bibliothèque et Archives nationales du Québec
Bibliothèque et Archives Canada, 2017

© Pelletier, Jabali, Laporte and CIRRELT, 2017

1. Introduction

Electric freight vehicles (EFVs) are fast becoming a viable alternative for short- and mid-haul goods distribution (Davis and Figliozzi 2013, Lee et al. 2013, Pelletier et al. 2016, Quak et al. 2016, Franceschetti et al. 2017). Because they help reduce air and noise pollution they are often regarded as an attractive option in the context of city logistics. Most recent studies have dealt with the routing issues associated with EFVs, especially those that result from their limited range, and have proposed models and algorithms for the optimization of routes that incorporate en route recharging (e.g., Felipe et al. 2014, Schneider et al. 2014, Bruglieri et al. 2015, Goeke and Schneider 2015, Hiermann et al. 2016, Montoya et al. 2017). Some authors have also approached such optimization problems from a more strategic planning perspective by incorporating both routing and charging infrastructure siting decisions in their models (e.g., Yang and Sun 2015, Schiffer and Walther 2015, 2016).

The issue of depot charge scheduling for electric vehicles has received less attention than the routing component, but it raises interesting problems whose solution could facilitate the integration of EFVs in goods distribution schemes. Indeed, most companies using EFVs prefer charging the vehicles at their own facilities because of a combination of factors (Naberezhnykh et al. 2012, Nesterova et al. 2013, E-Mobility NSR 2013). These include limited fast charging infrastructures in most regions, as well as long charging times associated with slow charging stations that lead to cargo security concerns and an ineffective use of drivers' time when charging during delivery routes. In addition, lower energy costs may be attained through commercial off-peak electricity rates when charging at the depot during specific periods of the day. Moreover, EFVs are more likely to be used in urban areas because of low driving speeds and frequent stop-and-starts, where their superior energy efficiency becomes relatively advantageous compared with that of diesel vehicles, and where financial incentives are more likely to be available. Typical urban delivery routes are shorter than the range of currently available EFVs (Feng and Figliozzi 2013), so there is often no need to consider charging outside the depot. While some studies have focused on charge scheduling for EFVs (e.g., Sassi and Oulamara 2014a,b), several important issues have not yet been addressed.

Before the publication of the recent paper by Montoya et al. (2017), charging was either treated as a fixed time penalty (e.g., Conrad and Figliozzi 2011, Afroditi et al. 2014, Preis et al. 2014), or was assumed to be linear with respect to time (e.g., Felipe et al. 2014, Schneider et al. 2014, Bruglieri et al. 2015, Lebeau et al. 2015, Goeke and Schneider 2015, Hiermann et al. 2016), which does not correspond to reality. Indeed, in order to prevent significant battery degradation resulting from operating the battery at voltage values beyond a specified value by the manufacturer, the charging function usually comprises both a linear and a non-linear component with respect to time. Moreover, certain charging practices of electric vehicles have been shown to adversely influence the lifespan of their batteries (Bashash et al. 2011, Lunz et al. 2012). Since the battery still remains a major cost component of EFVs (Pelletier et al. 2016), it becomes important to take this consideration into account when making charge scheduling decisions. This is indeed critical since high use rates have frequently been identified as a means to increase the cost competitiveness of EFVs because of their high purchase costs and low operational costs (Davis and Figliozzi 2013, Lee et al. 2013). However, recent studies (e.g., Taefi 2016, Taefi et al. 2016) have concluded that this may not be the case if costly battery replacements result from intensive usage in high utilization scenarios. In addition, such scenarios often involve using the vehicles in multi-shift contexts, whereby vehicles may need to perform multiple routes throughout day and night (EFVs are often allowed to perform night-time deliveries in cities because they are silent, Taefi 2016). In order to allow vehicles to complete their routes or benefit from off-peak electricity rates, such operational contexts may require expensive chargers at the depot in order to allow sufficient time to charge the vehicles between consecutive delivery routes during specific periods of the day. A company would probably own a limited number of chargers, typically fewer than the fleet size, thus requiring tight charging schedules.

Two relevant studies in this context are those of Sassi and Oulamara (2014a, 2014b). In the first of these papers, a fleet of electric and conventional vehicles must be assigned to a set of known tours so as to maximize the usage of the electric vehicles and minimize the cost of the charging schedule. Charging can only be performed at the depot when vehicles are not performing routes. The planning horizon is discretized into periods during which the charging power remains fixed and must be within a certain interval indicating the minimum and maximum charging power of the homogeneous chargers at the depot. Charging costs and grid capacities are time-dependent. Sassi and Oulamara (2014b) have extended this problem by considering different types of chargers at the depot and a limited number of each type. They also proposed different objective functions depending on whether certain considerations are taken into account or not. These include being allowed to exceed the grid capacity by paying certain penalties, the number of chargers of each type at the depot treated as a decision variables with deployment costs, and the presence of time-dependent greenhouse gas emissions costs depending on the electricty generation mix at that time.

Our work can be considered as an extension of these two studies. Indeed, as in Sassi and Oulamara (2014b), we focus on the depot charging schedule rather than on charging vehicles in public stations along delivery routes, but we model a more realistic charging process which avoids overcharging, and hence battery deterioration (Lam 2011). We also propose a continuous time formulation which may be used to generate more precise solutions than do discrete models in certain operational contexts. Moreover, we work with planning horizons of several days rather than with a single day, since the assumption that the vehicles can always be fully charged overnight between two routes does not hold in certain multi-shift operational contexts. In addition, we incorporate battery degradation considerations when determining the optimal charging schedule. Finally, we draw several managerial insights through our numerical experiments; such insights are relatively absent from the aforementioned related studies.

Our aim is to analyze charging schedules of EFVs that must deliver goods to a set of customers over the course of a multiple day planning horizon in a multi-shift operational context, thereby peforming multiple routes per day, and that can only be charged at a central depot. With this goal in mind, Section 2 describes the problem at hand and presents its initial mathematical formulation without battery degradation considerations. Section 3 explains how certain battery health considerations can be incorporated into the model. Section 4 proposes an alternate formulation that may be more appropriate in some specific operational contexts. Section 5 provides extensive computational results and derives managerial insights. The paper closes with conclusions in Section 6. Appendix A contains a glossary of the abbreviations used in the paper.

2. Problem Description

Our problem is defined over a planning horizon $[0, T_{max}]$ of several days which is discretized into set $P = \{1, ..., n_p\}$ of n_p equidistant periods, each having a duration of δ hours. The set $K = \{1, ..., m\}$ represents the fleet of m homogeneous EFVs. Each vehicle has a battery with a charge capacity of Q ampere-hours and an energy capacity of QE kWh. We define the state of charge (SOC) of a battery as the amount of charge it contains divided by its maximum charge capacity Q. The set R contains all delivery routes that must be performed over the planning horizon and are given as inputs. We assume that the assignment of vehicles to the delivery routes is also known in advance. Each route $r \in R$ is associated with the following parameters: a departure time DT_r in period DP_r, an arrival time AT_r in period AP_r, the vehicle v_r that must perform the route, the total SOC variation ΔSOC_r incurred by the vehicle performing it, and the earliest route η_r prior to it with $v_{\eta_r} = v_r$. Let f_k be the earliest route to be performed by vehicle k in the planning horizon, and let set A_k represent all periods during which vehicle k returns from one of its routes, i.e., $A_k = \{AP_r | r \in R, v_r = k\}$. Assume that $AP_{\eta_r} = 1$ and $AT_{\eta_r} = 0$ if $r = f_k$ for any vehicle $k \in K$.

At the depot, there is an energy cost of c_p in \$/kWh associated with each period $p \in P$ and a grid capacity G in kilowatts, the latter representing the maximum power that can be retrieved from the grid to charge the vehicles at any given moment. Indeed, depending on operational requirements, companies may be offered time-dependent energy costs for charging electric vehicles which are sometimes subject to maximum power restrictions (e.g., see Southern California Edison, 2017). We assume that there are different kinds of chargers installed at the depot, represented by the set S. A charger of type $s = 1$ is assumed to be a level 1 charger that comes with the vehicle upon its purchase; all vehicles can therefore use charger $s = 1$ whenever they are at the depot. The other chargers are faster but more costly. The acquisition, installation, and maintenance costs associated with such charging equipment are significant cost components of operating electric vehicles for goods distribution (Lee et al. 2013). It is therefore assumed that there is a limited number $\kappa_s < m$ of chargers of type $s \in S \backslash \{1\}$. The objective of the problem is to determine a charging schedule allowing the vehicles to complete all their routes at minimal cost.

2.1 Battery charging process

Electric vehicles are typically charged under a constant current (CC) - constant voltage (CV) scheme to avoid overcharging degradation (Lam 2011). The charging current (i.e., the rate of change of the SOC) is held constant during the CC phase and the SOC thus increases linearly with respect to time. During the CC phase, the terminal voltage of the battery increases until it reaches a certain maximum value. When it does, the CV phase begins and the terminal voltage must be maintained at that maximum value to avoid degradation resulting from overcharging the battery; the charging current then decreases with time.

The process can be quite easily understood through the Tremblay et al. (2007) model developed to represent battery behaviour. This model essentially states that the terminal voltage V_{term} of a battery is the sum of its open-circuit voltage OCV and the voltage drop across its internal resistance R, the latter term depending on the charging current i. The open-circuit voltage is the voltage measured at the battery terminals when it is at rest and is an increasing function of SOC. The terminal voltage is the voltage measured at the battery terminals when it is being charged or discharged and is a function of SOC and current. Using this simple circuit model, the terminal voltage during charging can be approximated as

$$V_{term}(SOC, i) = OCV(SOC) + R \cdot i. \tag{1}$$

The terminal voltage is thus larger than the open-circuit voltage during charging. During the CC phase of a CC-CV charging process, the charging current (which depends on the charger used) remains constant; the right-hand side of (1) therefore increases according to the relationship between open-circuit voltage and SOC, and thus so does the terminal voltage. As previously mentioned, the terminal voltage must never be allowed to go beyond a certain value V_{CV} specified by the manufacturer in order to avoid damaging the battery through overcharging. Depending on the charging current used during the CC phase, V_{CV} can be reached at SOC values well below 100%. In order to continue charging the battery once V_{CV} is reached, the terminal voltage must be held at that maximum value throughout the CV phase. Following an infinitesimal time increment after entering the CV phase, the SOC will then increase according to the current in the CC phase. Since the open-circuit voltage will increase with the SOC, the current will have to be decreased in order to ensure that the terminal voltage remains at V_{CV}. The process then repeats itself following other infinitesimal time increments until the battery is fully charged.

Note that the charging rate used in the CC phase influences both the elapsed time and the SOC upon entering the CV phase. Indeed, a larger current will shorten the CC phase but will cause the CV phase to be entered at a lower SOC value, thereby prolonging the CV phase. Figure 1 illustrates this process by simulating the CC-CV charging scheme for a 40Ah lithium-ion battery cell with different values for the current i_{CC} used during the CC phase and a maximum charge voltage V_{CV} of 3.6V. The final time T is the same in all simulations. As the value of i_{CC} increases, the time t_s at which the CV phase is entered decreases. However, the SOC at time t_s is approximately 87%, 85%, 81% and 74% when i_{CC} is 10A, 11A, 12A, and 13A respectively. It is also interesting to note that the SOC at time T remains relatively constant regardless of the value of i_{CC}.

In order to model the CC-CV process in discrete time, we use a piecewise linear approximation of the evolution of SOC over time, as in Montoya et al. (2017). Assume that each charger $s \in S$ has a specific CC-CV charging function that is piecewise linear with $b_s + 1$ breakpoints, fitted to the real CC-CV concave function. Let a_{si} be the SOC associated with breakpoint $i \in B_s$ of the charging function of charger $s \in S$, with $B_s = \{0, ..., b_s\}$ (the set of breakpoints). The approximation therefore assumes that the charging current is constant between each pair of consecutive breakpoints. Let I_{si} be the charging current used in the piecewise approximation between breakpoints i and $i-1$ of charger s, for all $i \in B_s \backslash \{0\}$, with I_{s1} therefore referring to the CC phase current of charger s.

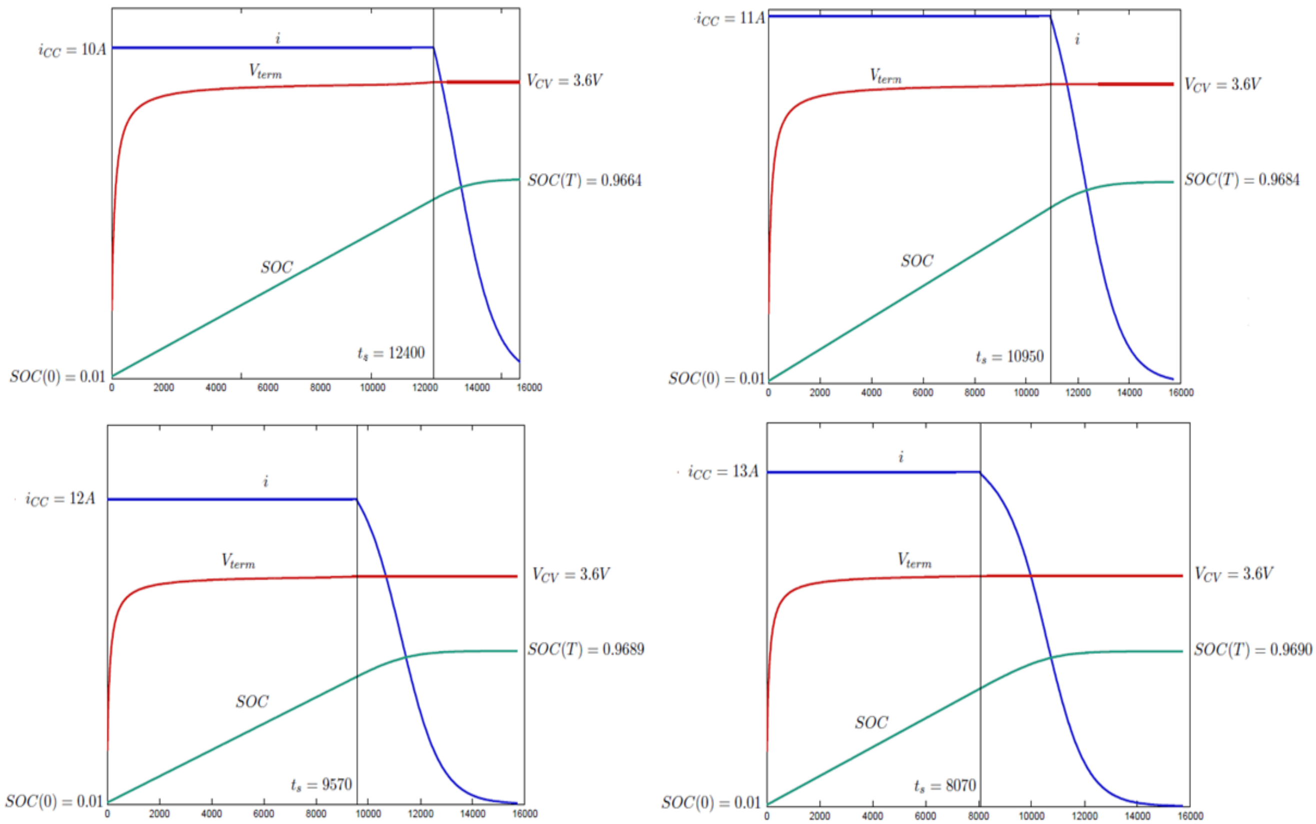

Figure 1: Comparison of CC-CV charging profile for a lithium-ion battery cell with different current values in the CC phase
Source: Pelletier et al. (2017)

Finally, note that the charging power applied to the battery during charging is equal to the product of its terminal voltage and of the charging current; it therefore increases with time during the CC phase of charging until it reaches a maximum value upon entering the CV phase, and then decreases throughout the CV phase. To ensure the respect of potential grid restrictions, let parameter P_s be the maximum charging power retrieved from the grid by the battery throughout the CC-CV charging process of charger s.

2.2 Mathematical formulation

Four sets of decision variables are required for the initial formulation of the problem. Real variables soc_{pk} refer to the state of charge of vehicle k at the start of period p, while real variables i_{pk} refer to the charging current applied to vehicle k during the entirety of period p. As in Sassi and Oulamara (2014a), we assume that the entire charge consumption of a route occurs during the last period of that route. For example, if vehicle $k = 1$ leaves the depot during period $p = 1$ with a SOC of 90%, and returns to the depot during period $p = 5$ with a SOC of 50%, the model is designed so that $SOC_{11} = SOC_{21} = SOC_{31} = SOC_{41} = 90\%$ and $SOC_{51} = 50\%$ (so the values of SOC_{pk} are irrelevant while the vehicle is performing its route; they remain the same as the departure SOC until the vehicle returns). Each vehicle starts with an initial SOC value (i.e., SOC_{1k} is a constant for each vehicle). We assume the SOC must remain between certain minimum and maximum values SOC_{min} and SOC_{max} for battery health reasons.

Binary variables x_{pksi} take value 1 if vehicle k uses a charger of type s during period p with SOC values at the start and end of p between breakpoints $a_{s,i-1}$ and a_{si}, and take value 0 otherwise. It is assumed that if a charger is used by a vehicle during a period, that charger is unavailable to other vehicles for the entirety of the period. Finally, binary variables z_{pk} take value 1 if vehicle k begins a new charge during period p and 0 otherwise. To avoid impractical solutions in which vehicles are constantly being moved from one charger to another, we set a limit of C charging events between each arrival and departure for all vehicles. We define a charging event as plugging a charger into a vehicle at a given time and unplugging it at a later time. The following mixed integer linear programming formulation then represents the problem at hand:

$$\text{minimize} \quad \sum_{k\in K}\sum_{p\in P}\frac{i_{pk}\cdot\delta}{Q}\cdot QE\cdot c_p \tag{2}$$

subject to

$$\sum_{p=DP_r}^{AP_r}\sum_{s\in S}\sum_{i\in B_s\setminus\{0\}} x_{pv_r si} = 0 \qquad r\in R \tag{3}$$

$$soc_{AP_r,v_r} = soc_{DP_r,v_r} - \Delta SOC_r \qquad r\in R \tag{4}$$

$$\sum_{k\in K}\sum_{i\in B_s\setminus\{0\}} x_{pksi} \le \kappa_s \qquad p\in P, s\in S\setminus\{1\} \tag{5}$$

$$\sum_{s\in S}\sum_{i\in B_s\setminus\{0\}} x_{pksi} \le 1 \qquad k\in K, p\in P \tag{6}$$

$$0 \le i_{pk} \le \sum_{s\in S}\sum_{i\in B_s\setminus\{0\}} x_{pksi}\cdot I_{si} \qquad k\in K, p\in P \tag{7}$$

$$soc_{p+1,k} \le a_{si} + 1 - x_{pksi} \qquad k\in K, p\in P\setminus\{n_p\}, s\in S, i\in B_s\setminus\{0\} \tag{8}$$

$$soc_{pk} \ge a_{s,i-1} - 1 + x_{pksi} \qquad k\in K, p\in P, s\in S, i\in B_s\setminus\{0\} \tag{9}$$

$$soc_{pk} = soc_{p-1,k} + \frac{i_{p-1,k}}{Q}\cdot\delta \qquad k\in K, p\in P\setminus\{1\}, p\notin A_k \tag{10}$$

$$SOC_{min} \leq soc_{pk} \leq SOC_{max} \qquad k \in K, p \in P \tag{11}$$

$$\sum_{k \in K} \sum_{s \in S} \sum_{i \in B_s \setminus \{0\}} x_{pksi} \cdot P_s \leq G \qquad p \in P \tag{12}$$

$$z_{pk} \geq \sum_{i \in B_s \setminus \{0\}} x_{pksi} - \sum_{i \in B_s \setminus \{0\}} x_{p-1,ksi} \qquad k \in K, p \in P \setminus \{1\}, s \in S \tag{13}$$

$$z_{1k} \geq \sum_{i \in B_s \setminus \{0\}} x_{1ksi} \qquad k \in K, s \in S \tag{14}$$

$$\sum_{p=AP_{\eta_r}+1}^{DP_r - 1} z_{pv_r} \leq C \qquad r \in R \tag{15}$$

$$x_{pksi} \in \{0, 1\} \qquad k \in K, s \in S, i \in B_s \setminus \{b_s\} \tag{16}$$

$$z_{pk} \in \{0, 1\} \qquad k \in K, p \in P. \tag{17}$$

The objective function (2) minimizes the total energy costs over the planning horizon. Our numerical simultations of the CC-CV process with the battery model of Tremblay et al. (2007) indicate that the cumulative energy (kWh) recharged in the battery is relatively constant regardless of the charging current used in the CC phase, and is linear with respect to SOC during the CC-CV process. We therefore compute the SOC variation during period p of vehicle k as the charging current i_{pk} (amperes) multiplied by the period length δ (hours) divided by the battery charge capacity Q (ampere-hours), and we then determine the corresponding energy recharged in the battery by multiplying the resulting SOC variation by the energy capacity QE (kWh).

Constraints (3) ensure that no charging takes place while a vehicle performs its route. We also assume that no charging can occur during departure and arrival periods. Constraints (4) set the SOC of each vehicle during the arrival period of each route to their SOC during the departure period of that route, minus the SOC consumption of the route. Constraints (5) state that for each charger type, at most the number of units installed of that type may be used by the fleet (not necessary for $s = 1$). Constraints (6) force each vehicle to use at most one charger per period. Constraints (7) ensure that the charging current applied to a vehicle during a period is at most the one associated with the segment of the CC-CV piecewise linear function (which depends on the charger used) within which it is being charged. Constraints (8) and (9) appropriately bound the SOC of each vehicle at the start and end of each period depending on the CC-CV piecewise linear function associated with the charger it is using. Constraints (10) link the SOC of a vehicle from one period to the next according the charging current (as long as it is not a period during which the vehicle returns from a route). Constraints (11) bound the SOC of each vehicle during each period. Constraints (12) ensure that the grid restriction is respected at all times. Constraints (13)–(15) mean that at most C charging events take place between each arrival and departure (or between the start of the horizon and the first route if $r = f_k$). Finally, constraints (16)–(17) define the domains of the variables not already appropriately bounded by the other constraints. Note that variables z_{pk} can also be treated as continuous.

3. Incorporating battery degradation considerations

Degradation occurs in electric vehicle batteries because of chemical and mechanical processes which ultimately lead to capacity and power fade (Barré et al. 2013). The degradation that occurs while cycling (i.e.,charging or discharging) the battery is referred to as cycle aging, while the degradation that occurs during storage is referred to as calendar aging. Battery degradation can either be estimated by using principles of electrochemistry, thereby modeling the reactions causing degradation within the battery, or by using a more empirical approach to predict battery aging according to experimental data (Bashash et al. 2011). Most transportation scientists would likely prefer a battery degradation model that can be understood without an expertise in electrochemisty and that can be calibrated with easily obtainable battery specifications without the need to perform experimental tests. Moreover, it seems desirable to have a model that translates battery degradation directly to monetary battery wear costs. For these reasons, we propose using the model of Han et al. (2014) to take into account cycle aging, followed by a possible second optimization phase to mitigate calendar aging when necessary. The latter is dicussed in Section 5.4, while the former is discussed in what follows.

3.1 Cycle aging model

Requiring only the battery's acquisition cost and cycle life versus depth of discharge (DOD) data typically provided in the data sheets, Han et al. (2014) proposed a function representing wear costs per unit of energy going in or out of the battery according to the battery's SOC in order to account for different degradation rates occurring at different SOC values. Manufacturers typically provide what Han et al. (2014) refer to as the ACC-DOD curve (Achievable Cycle Count as a function of DOD), which indicates how many cycles the battery will be able to perform at that DOD before it reaches the end of its lifetime, assuming the battery is always discharged starting from a SOC of 1. For example, at a DOD of 0.4, the ACC-DOD curve would indicate the number of times the battery can be discharged from a SOC of 1 to a SOC of 0.6 and then charged back to 1 before the end of its lifespan. The problem, however, is that in reality the battery will be cycled over different SOC ranges over its lifespan and at different SOC points (e.g., a DOD of 0.4 could be from 1 to 0.6, but also from 0.7 to 0.3, which would cause a different wear on the battery).

Acknowledging this fact, the Han et al. (2014) model attributes a cost per kilowatt-hour charged or discharged as a function of SOC based on the ACC-DOD data provided by the manufacturer. The authors propose a method for determining the wear cost function in both a continuous and discrete manner. The discrete version can be derived as follows. Let function $ACC(D)$ refer to the ACC-DOD curve, i.e., $ACC(D)$ indicates how many times the battery can be discharged from a SOC of 1 to a SOC of $1 - D$, and then charged back from a SOC of $1 - D$ to a SOC of 1. For the discrete version of the model, only a finite number of points from the ACC-DOD curve are required, and the SOC is discretized into corresponding intervals of length ΔSOC. The wear cost function $W(SOC)$ then indicates the cost per kWh charged or discharged in the SOC interval $[SOC, SOC + \Delta SOC]$ and satisfies

$$\text{Battery price} = 2 \cdot ACC(D) \cdot \sum_{SOC=1-D}^{1-\Delta SOC} (W(SOC) \cdot \Delta q), \tag{18}$$

where Δq is the quantity of energy (kWh) in each SOC interval. Equation (18) must hold for each value of D used from the ACC-DOD curve. For example, if the manufacturer's ACC-DOD curve only provides points separated by 10% DOD intervals (or if the user wants the wear cost function for SOC intervals of 10%), the following ten equations (which are easy to solve) can be used to calibrate the wear cost function:

$$\begin{aligned}
W(0.9) &= \frac{\text{Battery price}}{ACC(0.1) \cdot 2 \cdot \Delta q} \\
W(0.8) + W(0.9) &= \frac{\text{Battery price}}{ACC(0.2) \cdot 2 \cdot \Delta q} \\
\vdots \qquad & \qquad \vdots \\
W(0) + ... + W(0.9) &= \frac{\text{Battery price}}{ACC(1) \cdot 2 \cdot \Delta q}.
\end{aligned}$$

In Han et al. (2014), the wear model is applied in a vehicle-to-grid optimization problem using particle swarm optimization. In what follows we propose methodologies for incorporating the battery wear function in a tractable way for commercial solvers. The wear cost function used in the original paper increases with SOC (i.e., cycling the battery in higher SOC intervals is more detrimental to the battery than in SOC intervals), but the authors point out that this should not be considered as a universal characteristic of electric vehicle batteries.

3.1.1 Monotonic wear cost functions

In the case of monotonic wear costs with respect to SOC, the degradation costs can be incorporated as follows. Let $D = \{1, ..., n_d\}$ represent the set of n_d SOC intervals used to calibrate the discrete wear cost function, with each interval $d \in D$ characterized by a lower SOC bound $\underline{S}_d$ and an upper SOC bound $\overline{S}_d$. Let W_d be the wear cost per kilowatt-hour charged and discharged in the SOC interval d, and L be the length of each SOC interval in D. Define real variables Δsoc_{dr} as the quantity of SOC interval $d \in D$ charged into vehicle v_r between arriving from route η_r (or the start of the horizon if $r = f_{v_r}$) and leaving for route r. Binary variables u_{dr} are permitted to take a value of 1 if interval d can be used to charge vehicle v_r between arriving from route η_r (or the start of the horizon if $r = f_{v_r}$) and leaving for route r. Then the following constraints need to be added to the problem regardless of whether the wear cost function is non-decreasing or non-increasing:

$$\sum_{d \in D} \Delta soc_{dr} = soc_{DP_r, v_r} - soc_{AP_{\eta_r}, v_r} \quad r \in R \tag{19}$$

$$0 \le \Delta soc_{dr} \le L \cdot u_{dr} \quad d \in D, r \in R. \tag{20}$$

Constraints (19) ensure that for each vehicle, the sum of all SOC intervals in D between arriving from a route and leaving for its next route is equal to the total SOC variation resulting from charging the vehicle between arriving from the first route and leaving for the next. Constraints (20) state that the amount used in each SOC interval is at most L if that interval is allowed to be used, and 0 otherwise.

If the wear function is non-decreasing with SOC, then more degradation is incurred by cycling the battery in higher SOC intervals. Then the following constraints should be added to the problem in addition to constraints (19)–(20):

$$\Delta soc_{dr} \le \overline{S}_d - soc_{AP_{\eta_r}, v_r} + 1 - u_{dr} \quad d \in D, r \in R. \tag{21}$$

Indeed, (21) ensures that the variables u_{dr} can only take a value of 1 for SOC intervals with an upper bound that is larger than the SOC of vehicle v_r upon arriving from the previous route (or its SOC at the start of the horizon if it is the vehicle's first route). Since the wear costs increase with SOC in this case, the model will always automatically fill out all lower SOC intervals, with the lowest admissible interval being bounded by the difference between its upper bound and the SOC of the vehicle upon arriving from its previous route rather than by the interval length L. Similarly, if the wear cost function is non-increasing with respect to SOC, then more degradation is incurred by cycling the battery at lower SOC values. Then the following constraints should be added to the problem in addition to constraints (19)–(20):

$$\Delta soc_{dr} \leq soc_{DP_r,v_r} - \underline{S}_d + 1 - u_{dr} \quad d \in D, r \in R \tag{22}$$

since in this case the model will always want to fill out all higher SOC intervals first, with the highest admissible interval being bounded by the difference between its lower bound and the departure SOC of the upcoming route rather than by the interval length L. Finally, in both cases, the objective function (2) should be replaced with

$$\text{minimize} \quad \sum_{k \in K} \sum_{p \in P} \frac{i_{pk} \cdot \delta}{Q} \cdot QE \cdot c_p + \sum_{r \in R} \sum_{d \in D} QE \cdot \Delta soc_{dr} \cdot W_d. \tag{23}$$

3.1.2 General wear cost functions

If the wear function is not monotonic, then the model cannot be expected to fill out all lower or upper intervals first with the approaches suggested in the Section 3.1.1. However, since the wear cost is always constant in a given SOC interval $d \in D$, a cumulative wear cost function can be represented as a piecewise linear function of SOC. A point at a given SOC in this cumulative wear cost function would indicate the total wear costs incurred for charging the battery from 0 to that SOC. We use the approach of Montoya et al. (2017) to model the cumulative wear cost function. The idea is essentially to determine initial and final positions on a piecewise linear function by constructing convex combinations of the function's breakpoints.

Let ζ_{dr} be a binary variable equal to 1 if the SOC of vehicle v_r is between $\overline{S}_{d-1}$ and $\overline{S}_d$ upon arriving from route η_r or at the start of the horizon if $r = f_{v_r}$, with $\overline{S}_0 = \underline{S}_1$. Similarly, let ψ_{dr} be a binary variable equal to 1 the SOC of vehicle v_r is between $\overline{S}_{d-1}$ and $\overline{S}_d$ upon leaving for route r. Let ϵ_{dr} and w_{dr} be the coefficients of breakpoint $\overline{S}_d$ used in the convex combinations to determine the position of vehicle v_r on the cumulative wear function when arriving from η_r (or the start of the horizon if $r = f_{v_r}$) and leaving for r respectively. Let cs_r and ce_r be the starting and ending cost positions of vehicle v_r on the cumulative wear function when arriving from η_r (or the start of the horizon if $r = f_{v_r}$) and leaving for r respectively. Let C_d be the cummulative wear cost in the piecewise linear function at breakpoint $\overline{S}_d$, for all $d \in D \cup \{0\}$. Then any discrete wear cost function can be incorporated into the charge scheduling problem with the following constraints:

$$\sum_{d \in D \cup \{0\}} \epsilon_{dr} = \sum_{d \in D} \zeta_{dr} = 1 \quad r \in R \tag{24}$$

$$\sum_{d \in D \cup \{0\}} w_{dr} = \sum_{d \in D} \psi_{dr} = 1 \quad r \in R \tag{25}$$

$$soc_{AP_{\eta_r}, v_r} = \sum_{d \in D \cup \{0\}} \epsilon_{dr} \cdot \overline{S}_d \quad r \in R \tag{26}$$

$$soc_{DP_r, v_r} = \sum_{d \in D \cup \{0\}} w_{dr} \cdot \overline{S}_d \quad r \in R \tag{27}$$

$$cs_r = \sum_{d \in D \cup \{0\}} v_{dr} \cdot C_d \quad r \in R \tag{28}$$

$$ce_r = \sum_{d \in D \cup \{0\}} w_{dr} \cdot C_d \quad r \in R \tag{29}$$

$$\epsilon_{0r} \leq \zeta_{1r} \quad r \in R \tag{30}$$

$$\epsilon_{dr} \leq \zeta_{dr} + \zeta_{d+1,r} \quad r \in R, d \in D \backslash \{n_d\} \tag{31}$$

$$\epsilon_{n_d,r} \leq \zeta_{n_d,r} \quad r \in R \tag{32}$$

$$w_{0r} \leq \psi_{1r} \quad r \in R \tag{33}$$

$$w_{dr} \leq \psi_{dr} + \psi_{d+1,r} \quad r \in R, d \in D \backslash \{n_d\} \tag{34}$$

$$w_{n_d,r} \leq \psi_{n_d,r} \quad r \in R \tag{35}$$

$$\zeta_{dr}, \psi_{dr} \in \{0, 1\} \quad r \in R, d \in D \tag{36}$$

$$\epsilon_{dr}, w_{dr} \geq 0 \quad r \in R, d \in D \cup \{0\}. \tag{37}$$

Constraints (24)–(25) force the SOC values upon arriving from a route (or at the start of the horizon) and leaving for the next route to be between two of the SOC breakpoints of the cumulative wear function, and force the sum of the breakpoint coefficients to be equal to 1. Constraints (24)–(27) and (37) together force the SOC values upon arriving from a route (or at the start of the horizon) and leaving for the next route to be convex combinations of the SOC breakpoints of the cumulative wear cost function. Constraints (28)–(29) determine the costs on the cumulative wear function corresponding to these convex combinations. Constraints (30)–(35) force these convex combinations to only use two consecutive breakpoints of the cumulative wear cost function. Constraints (36)–(37) define the domain of the new variables. Finally, in this case, the objective function (2) should be replaced with

$$\text{minimize} \quad \sum_{k\in K}\sum_{p\in P}\frac{i_{pk}\cdot\delta}{Q}\cdot QE\cdot c_p+\sum_{r\in R}(ce_r-cs_r). \tag{38}$$

4. Model extension to continuous time

The formulation in discrete time has the advantage of easily handling time-dependent energy costs and grid restrictions. However, if energy costs are constant throughout the day and the grid capacity is non-binding, the problem can be modeled in continuous time, which can provide more precision in the charging schedule since the discrete time model works with charger availability on a period to period basis rather than a minute to minute basis.

In order to model charger availability in continuous time, we introduce binary parameter Γ_{r_1,r_2} for all $r_1, r_2 \in R|v_{r_1} \neq v_{r_2}$. Parameter Γ_{r_1,r_2} takes value 1 if $[AT_{\eta_{r_1}}, DT_{r_1}] \cup [AT_{\eta_{r_2}}, DT_{r_2}] \neq \emptyset$, i.e., if there exists an interval of time during which vehicles v_{r_1} and v_{r_2} are both at the depot between arriving from routes η_{r_1} (or the start of the horizon if $r_1 = f_{v_{r_1}}$) and η_{r_2} (or the start of the horizon if $r_2 = f_{v_{r_2}}$) respectively, and leaving for routes r_1 and r_2 respectively. We refer to the interval of time $[AT_{\eta_r}, DT_r]$ as charging opportunity r, i.e., the interval of time during which vehicle v_r can recharge between routes η_r and r. Consider set $U = \{1, ..., C\}$ to represent the charging events that can occur at each charging opportunity. For each charging opportunity, if $u_1, u_2 \in U$ with $u_2 > u_1$, we force charging event u_2 to take place after charging event u_1. We also redefine set S to represent each individual charger that is installed at the depot, rather than to represent the types of charger as in the discrete time model (i.e., $s \in S$ now refers to a specific charger rather than to a type of charger; the only exception is $s = 1$, which still represents all level 1 chargers).

Let real variables λ_{ur} represent the start time of the u^{th} charge of charging opportunity r. Let real variables ρ_{ur} represent the end time of the u^{th} charge of charging opportunity r. Let binary variables x_{usr} take value 1 if the u^{th} charge of charging opportunity r takes place with charger s. Let real variables $socB_{ur}$ and $socE_{ur}$ represent the SOC at the start and at the end of the u^{th} charge of charging opportunity r. The SOC of each vehicle k at the start of the horizon, i.e., $socB_{1,f_k}$, is some known constant. Let L_k be the last route of the horizon to be performed by vehicle k; then variables $socB_{ur}$ must also be defined for $u = 1$ and fictional routes $r_k \quad \forall k \in K$, with $\eta_{r_k} = L_k$ in order to represent the SOC of vehicle k upon returning from its last route. Let R_L contain all such fictional routes. Let binary variables $\chi_{utsr_1r_2}$ take value 1 if $\Gamma_{r_1,r_2} = 1$ and if the u^{th} charge of charging opportunity r_1 and the t^{th} charge of charging opportunity r_2 are done with charger $s \in S\backslash\{1\}$, with the u^{th} of r_1 occuring after the end of the t^{th} of r_2.

In this model we use the same approach as Montoya et al. (2017) to model the piecewise linear approximation of the CC-CV charging process in continuous time, similarly to what was done for general wear cost functions in Section 3.1.2. As previously mentioned, assume that each charger $s \in S$ has a specific CC-CV charging function that is piecewise linear with $b_s + 1$ breakpoints, fitted to the real CC-CV concave function. Let a_{si} and h_{si} be the SOC and the charging time associated with breakpoint $i \in B_s$ of the charging function of charger $s \in S$, with $B_s = \{0, ..., b_s\}$ (the set of breakpoints). For a given breakpoint $i \in B_s$, h_{si} thus indicates the time required to charge the battery from a SOC of 0 to a SOC of a_{si}.

Let θ_{usri} be a binary variable equal to 1 if vehicle v_r uses charger s for the u^{th} charge of charging opportunity r and its SOC is between $a_{s,i-1}$ and a_{si} at the start of that charge. Similarly, let σ_{usri} be a binary variable equal to 1 if v_r uses charger s for the u^{th} charge of charging opportunity r, and its SOC is between $a_{s,i-1}$ and a_{si} at the end of that charge. Let π_{usri} and β_{usri} be the coefficients of breakpoint $i \in B_s$ used to determine the initial and final positions on the charging function of charger s for the u^{th} charge of charging opportunity r, if this charge is done with charger s. Finally, let st_{ur} and en_{ur} be the initial and final time positions on the charging function of charger s for the u^{th} charge of charging opportunity r, if this charge is done with charger s.

The mixed integer linear programming formulation of the problem in continuous time with constant energy costs and no grid capacity constraints is then the following:

$$\text{minimize} \quad \sum_{r \in R} (socE_{C,r} - socB_{1r}) \cdot QE \cdot c \tag{39}$$

subject to

$$socB_{1,r_2} = socE_{C,r_1} - \Delta SOC_{r_1} \quad r_1 \in R, r_2 \in R \cup R_L, \eta_{r_2} = r_1 \tag{40}$$

$$socB_{ur} = socE_{u-1,r} \qquad r \in R, u \in U\backslash\{1\} \tag{41}$$

$$\rho_{tr_2} \leq \lambda_{ur_1} + M \cdot (3 - x_{usr_1} - x_{tsr_2} - \chi_{utsr_1r_2}) \qquad \begin{array}{l} u, t \in U; s \in S\backslash\{1\}; \\ r_1, r_2 \in R, \Gamma_{r_1,r_2} = 1, v_{r_1} > v_{r_2} \end{array} \tag{42}$$

$$\rho_{ur_1} \leq \lambda_{tr_2} + M \cdot (2 - x_{usr_1} - x_{tsr_2} + \chi_{utsr_1r_2}) \qquad \begin{array}{l} u, t \in U; s \in S\backslash\{1\}; \\ r_1, r_2 \in R, \Gamma_{r_1,r_2} = 1, v_{r_1} > v_{r_2} \end{array} \tag{43}$$

$$AT_{\eta_r} \leq \lambda_{ur} \leq \rho_{ur} \leq DT_r \qquad r \in R, u \in U \tag{44}$$

$$\lambda_{ur} \geq \rho_{u-1,r} \qquad r \in R, u \in U\backslash\{1\} \tag{45}$$

$$\sum_{s \in S} x_{usr} = 1 \qquad r \in R, u \in U \tag{46}$$

$$SOC_{min} \leq socB_{ur} \leq socE_{ur} \leq SOC_{max} \qquad r \in R, u \in U \tag{47}$$

$$\rho_{ur} - \lambda_{ur} = en_{ur} - st_{ur} \qquad r \in R, u \in U \tag{48}$$

$$\sum_{i \in B_s} \pi_{usri} = \sum_{i \in B_s\backslash\{0\}} \theta_{usri} = x_{usr} \qquad r \in R, u \in U, s \in S \tag{49}$$

$$\sum_{i \in B_s} \beta_{usri} = \sum_{i \in B_s\backslash\{0\}} \sigma_{usri} = x_{usr} \qquad \in R, u \in U, s \in S \tag{50}$$

$$socB_{ur} = \sum_{s \in S} \sum_{i \in B_s} \pi_{usri} \cdot a_{si} \qquad r \in R, u \in U \tag{51}$$

$$socE_{ur} = \sum_{s \in S} \sum_{i \in B_s} \beta_{usri} \cdot a_{si} \qquad r \in R, u \in U \tag{52}$$

$$st_{ur} = \sum_{s \in S} \sum_{i \in B_s} \pi_{usri} \cdot h_{si} \qquad r \in R, u \in U \tag{53}$$

$$en_{ur} = \sum_{s \in S} \sum_{i \in B_s} \beta_{usri} \cdot h_{si} \qquad r \in R, u \in U \tag{54}$$

$$\pi_{usr0} \leq \theta_{usr1} \qquad r \in R, u \in U, s \in S \tag{55}$$

$$\pi_{usri} \leq \theta_{usri} + \theta_{usr,i+1} \qquad r \in R, u \in U, s \in S, i \in B_s\backslash\{0, b_s\} \tag{56}$$

$$\pi_{usr,b_s} \leq \theta_{usr,b_s} \qquad r \in R, u \in U, s \in S \tag{57}$$

$$\beta_{usr0} \leq \sigma_{usr1} \qquad r \in R, u \in U, s \in S \tag{58}$$

$$\beta_{usri} \leq \sigma_{usri} + \sigma_{usr,i+1} \qquad r \in R, u \in U, s \in S, i \in B_s\backslash\{0, b_s\} \tag{59}$$

$$\beta_{usr,b_s} \leq \sigma_{usr,b_s} \qquad r \in R, u \in U, s \in S \tag{60}$$

$$\theta_{usri}, \sigma_{usri} \in \{0, 1\} \qquad r \in R, u \in U, s \in S, i \in B_s\backslash\{0\} \tag{61}$$

$$\pi_{usri}, \beta_{usri} \geq 0 \qquad r \in R, u \in U, s \in S, i \in B_s \tag{62}$$

$$\chi_{utsr_1r_2} \in \{0,1\} \quad u, v \in U; s \in S \backslash \{1\}, r_1, r_2 \in R, \Gamma_{r_1,r_2} = 1, v_{r_1} > v_{r_2} \tag{63}$$

$$x_{usr} \in \{0,1\} \qquad r \in R, u \in U, s \in S. \tag{64}$$

The objective function (39) minimizes the sum of energy costs over the horizon, with c referring to the constant energy cost. Constraints (40) adjust the SOC of vehicles upon arriving from a route according to their SOC upon departing for the route and the SOC consumption of the route. Constraints (41) link the SOC at the start of each charge of a charging opportunity to the one at the end of the previous charge in that charging opportunity. Constraints (42) and (43) ensure that two vehicles never use the same charger at the same time, with M being an appropriate large constant, e.g., $M = DT_{r_1} - AT_{\eta_{r_1}} + DT_{r_2} - AT_{\eta_{r_2}}$. Note that these constraints are not required for charges done with $s = 1$ since each vehicle has a level 1 charger. Constraints (44) set the time interval defining each charging opportunity. Constraints (45) ensure that during each charging opportunity, the first charge ends before the second begins, the second ends before the third begins, and so on. Constraints (46) force one charger to be chosen per charge, but this does not prevent a charge from having a length of zero and thus being inexistent (so $s = 1$ can always be chosen without preventing other vehicles from using any other chargers). Constraints (47) ensure that the starting SOC is never higher than the ending SOC and bounds these appropriately. Constraints (48) set the difference between the ending and beginning of each charge according to the initial and final time positions on the charging function used for that charge. Constraints (49)–(50) link the π_{usri}, β_{usri}, θ_{usri}, σ_{usri} to the x_{usr} variables. Constraints (49)–(52) together force the starting and ending SOC of each charge to be a convex combination of the SOC breakpoints of whichever charger was chosen for that charge. Constraints (53) and (54) force the starting and ending times of each charge to be convex combinations of the time breakpoints of the charging function of whichever charger was chosen for that charge. Constraints (55)–(57) force the convex combination determining the starting SOC and time of each charge to only use two consecutive breakpoints of the function of the chosen charger. Constraints (58)–(60) force the convex combination determining the ending SOC and time of each charge to only use two consecutive breakpoints of the function of the chosen charger. Finally, constraints (61)–(64) define the domains of all variables not already appropriately bounded elsewhere in the model.

Battery wear costs can be added to the continuous time model as was done in the discrete time model. For monotonic wear functions, it suffices to add variables Δsoc_{dr} for SOC interval d and charging opportunity r, indicating how much of SOC interval d was charged into vehicle v_r during charging opportunity r, and binary variables u_{dr} which can take a value of 1 only if interval $d \in D$ could potentially be charged during charging opportunity r. The battery degradation costs can then be incorporated in the continuous time models by adding the constraints

$$\sum_{d \in D} \Delta soc_{dr} = socE_{Cr} - socB_{1r} \quad r \in R \tag{65}$$

$$0 \leq \Delta soc_{dr} \leq L \cdot u_{dr} \quad d \in D, r \in R. \tag{66}$$

If the wear cost function is non-decreasing with respect to SOC, then the following constraints should be added to the problem in addition to constraints (65)–(66):

$$\Delta soc_{dr} \leq \overline{S}_d - socB_{1r} + 1 - u_{dr} \quad d \in D, r \in R. \tag{67}$$

If the wear function is non-increasing with respect to SOC, then the following constraints should be added to the problem in addition to constraints (65)–(66):

$$\Delta soc_{dr} \leq socE_{Cr} - \underline{S}_d + 1 - u_{dr} \quad d \in D, r \in R. \tag{68}$$

In both cases of monotonic wear functions, the objective function (39) of the continuous time models should be replaced with

$$\text{minimize} \quad \sum_{d \in D} \sum_{r \in R} \Delta soc_{dr} \cdot QE \cdot (c + W_d). \tag{69}$$

In the case of general wear functions, the same approach as in Section 3.1.2 can be used by replacing arrival and departing SOC variables for each pair of consecutive routes of each vehicle by the starting SOC of the first charge and the ending SOC of the last charge of each charging opportunity.

4.1 Deriving an equivalent solution in continuous time from the discrete time model

Note that in order to use an equality in constraints (10), we allow the charging current i_{pk} in constraints (7) of the discrete time model to be less than the value I_{si} associated with the segment of the CC-CV piecewise linear function vehicle k is using during period p. Therefore, this may result in solutions in which certain charging events do not represent a CC-CV process in continuous time. In other words, the current could go up and down from one period to the next even if the SOC remains between the same two breakpoints. However, we mention here, as a side note, that a feasible solution that respects the CC-CV process in continuous time can always be constructed from the solution obtained in discrete time. Indeed, whenever i_{pk} does not take the maximum value it could during any period of a charging event, the same SOC variation from that charging event could be obtained within less time with the CC-CV process in continuous time.

Moreover, assuming such a solution (i.e., within which i_{pk} does not always take the maximum value it could during a charging event), as long as the function representing energy costs with respect to time during the charging event is quasiconvex or monotonic, the same energy costs as those in the discrete time solution can be obtained with the CC-CV process in continuous time for that charging event without having to split it into multiple events (i.e., disconnect and reconnect the charging chord at some point). If the function representing energy costs with respect to time over the course of the charging event is not monotonic but quasiconcave, then the same energy costs can be obtained by disconnecting and reconnecting the chord at most once (i.e., splitting the charging event in two). Since time of use energy plans often involve two or three rates over the course of a full day (e.g., mid-peak in the morning, peak during the afternoon, mid-peak in the evening, off-peak at night, with peak rate > mid-peak rate > off-peak rate), it seems unlikely that the function of energy costs with respect to time would not be monotonic, quasiconvex, or quasiconcave during a charging event. In addition, some charger manufacturers (e.g., eMotorWerks, 2017) are even starting to offer products allowing the beginning and termination of charging at specific times without having to unplug and plug the chord. In this case the same energy costs can be obtained in continuous time regardless of the shape of the function of energy costs with respect to time during the charging event.

Finally, since the grid capacity constraints (12) in discrete time are modeled assuming the maximum charging power of each charger, any modification of a charging event in discrete time to obtain an equivalent solution in continuous time will also respect the grid restriction in continuous time.

5. Numerical experiments and managerial insights

We have performed an extensive numerical study in order to gain numerical and managerial insights into our models. More precisely, the aims of our experiments are: (1) to validate the proposed formulations, (2) to investigate the trade-off that exists between energy and degradation costs, (3) to investigate the impact of grid restrictions on costs, (4) to analyze the effect of facilities related demand (FRD) charges, which are fees based on the maximum registered charging power over the planning horizon, (5) to shed light on the importance of calendar aging considerations in certain contexts, and (6) to examine the effect of costs related to the depot charging infrastructure.

To this end, we generated several test instances and we solved them under various scenarios. All test instances were solved using CPLEX 12.6 with a time limit of five hours and an optimality gap tolerance of 0.5%. We use a higher optimality gap tolerance than the default setting for two reasons. First, several parameter approximations are required regarding charging functions, energy recharged in the batteries, and degradation costs. Second, our goal with these experiments is not to demonstrate the computational prowess of the models, but rather derive meaningful managerial insights from reasonably good solutions. Aside from some of the experiments in Sections 5.1.1 and 5.6 that also optimize the charging infrastructure, as well as a few experiments in Section 5.3 when FRD charges are added to the problem, all tests generate a solution with an optimality gap under 0.5% within the time limit.

Davis and Figliozzi (2013) report that scenarios in which the daily distances traveled by electric trucks approach their maximum range can significantly help their business case. We therefore assume that the vehicles discharge at least 80% of their battery on a daily basis as high vehicle utilization scenarios. Two different operational contexts allowing such high use rates were initially considered. In the first, all vehicles in the fleet must perform one day-time route and one night-time route during each day of the planning horizon. In the second, all vehicles in the fleet only perform day-time routes. For each of these contexts, we worked with a planning horizon of three days, with period lengths of thirty minutes, and we considered fleets of five, 10 and 15 vehicles.

The fleet vehicles are assumed to be medium-duty electric trucks equiped with 80kWh batteries, each consisting of several 3.2V-40Ah lithium-ion battery cells. We set SOC_{min} to 0.05 and SOC_{max} to 0.99 for battery health reasons. Using some battery modeling considerations detailed in Pelletier et al. (2017) with battery parameters from Marra et al. (2012), we conducted numerical simulations of the CC-CV charging process for such battery cells with a maximum charge voltage of 3.65V and three different charging currents during the CC phase: 2.5A, 7.5A, and 17.5A. We consider the 2.5A to correspond to level 1 chargers (i.e., each vehicle has one). With this charger, the batteries can be fully charged from SOC_{min} to SOC_{max} in approximately 15 hours. The CV process is entered at a SOC of 0.98, so we simply approximate the entire CC-CV process with two breakpoints: 0.05 and 0.99. With the 7.5A charger, the batteries can be fully charged from SOC_{min} to SOC_{max} in 5.3 hours. The CV process is entered at a SOC of 0.95 after 4.8 hours, and we approximate the CC-CV process with three SOC breakpoints: 0.05, 0.95, and 0.99. The charging currents used in our piecewise approximation for this charger are 7.5A between 0.05 and 0.95, and 3.2A between 0.95 and 0.99. Finally, with the 17.5A charger, the batteries can be fully charged from SOC_{min} to SOC_{max} in 2.7 hours. The CV process is entered at a SOC of 0.78 and we approximate the CC-CV process associated with this charger with four breakpoints: 0.05, 0.78, 0.95, and 0.99. The charging currents used in our piecewise approximation for this charger are 17.5A between 0.05 and 0.78, 13.6A between 0.78 and 0.95, and 3.2A between 0.95 and 0.99. In all tested instances, we let each vehicle perform two charging events (i.e., $C = 2$) between each pair of consecutive routes in order to allow combining the use of the slow level 1 chargers with a faster charger.

We use time-dependent energy costs offered by Southern California Edison (2017) for businesses charging electric vehicles on company grounds. Two different plans (TOU-EV-3 and TOU-EV-4) are available depending on the maximum charging power retrieved from the grid at any given moment. Under the TOU-EV-3 rate plan, the maximum power retrieved from the grid for charging the vehicles must remain below 20kW, while under the TOU-EV-4 plan, the maximum charging power must remain under 500kW. Our simulations of the CC-CV charging process indicate that approximately 600 of the considered battery cells would need to be connected to form the battery pack so that a full charge from SOC_{min} to SOC_{max} corresponds to 80kWh put into the battery, resulting in maximum pack charging powers of approximately 5kW for 2.5A charger, 15 kW for the 7.5A, and 35kW for the 17.5A. We therefore assume that grid capacity constraints under these circumstances can be ignored with the TOU-EV-4 plan.

The energy prices under both plans vary with time of day and season. Peak hours are from noon to 18:00, mid-peak hours are from 8:00 to noon and from 18:00 to 23:00, and off-peak hours are from 23:00 to 8:00. Summer rates are in place from the first Saturday of June to the first Saturday of October, while winter rates apply for the rest of the year. There are also two different options under the TOU-EV-3 plan: option A has higher energy rates but no FRD charges, while option B has lower energy rates but FRD charges. FRD charges are monthly fees based on the maximum charging power retrieved from the grid throughout the month. The TOU-EV-4 plan also has FRD charges. We initially disregard this fee and subsequently study its impact in Section 5.2. The energy rates and FRD charges of each plan are summarized in Table 1.

Table 1: Rates ($/kWh) and FRD charges ($/kW) for electric vehicle charging on company grounds

	TOU-EV-4		TOU-EV-3-A		TOU-EV-3-B	
	Summer	Winter	Summer	Winter	Summer	Winter
Peak	0.29	0.11	0.36	0.16	0.33	0.12
Mid-peak	0.12	0.09	0.17	0.14	0.14	0.11
Off-peak	0.05	0.06	0.09	0.10	0.06	0.07
FRD charges	13.20	13.20	N/A	N/A	7.23	7.23

Regarding battery degradation, we first consider a battery wear cost function calibrated with the same cycle life data used in the original paper of Han et al. (2014), resulting in a non-decreasing wear cost function. It is therefore preferable to avoid cycling such a battery in high SOC values. We calibrate the degradation costs for SOC intervals of 25% assuming battery costs of $600/kWh as in Goeke and Schneider (2015) and thus a battery price of $48,000 (i.e., $\frac{\$600}{\text{kWh}} \cdot 80\text{kWh}$). We also multiply the obtained wear costs by two, since they represent $/kWh charged or discharged in each SOC interval, and anything charged in any solution to our problem will necessarily be subsequently discharged while performing the routes. The resulting costs are reported in Table 2.

Table 2: Battery wear cost function

SOC interval	Degradation costs
0–0.25	$0.64/kWh
0.25–0.5	$0.71/kWh
0.5–0.75	$0.87/kWh
0.75–1	$1.09/kWh

5.1 Different high-use rate contexts

For each of the two operational contexts allowing high use rates of the vehicles, we generate five test instances for fleet sizes of five, 10, and 15 vehicles. The planning horizon begins at 6:00 and each vehicle is then assumed to have a SOC of 0.5.

For the high use rate context in which each vehicle in the fleet has one day-time route and one night-time route to perform each day, it is assumed all day-time routes occur between 10:00 and 18:00, and all night-time routes occur between 22:00 and 6:00. The departure time of each route is randomly generated between 10:00 and 13:00 for each day-time route, and between 22:00 and 1:00 for each night-time route. Similarly, the arrival time of each route is randomly generated between 15:00 and 18:00 for each day-time route, and between 3:00 and 6:00 for each night-time route. The SOC consumption of each route is randomly generated between 0.45 and 0.90.

For the operational context in which vehicles only perform routes during the day-time, we assume vehicles should use at least 80% of the battery capacity each day. We assume each vehicle performs two short routes per day, with the first route occuring between 8:00 and 13:00, and the second route occuring between 15:00 and 20:00. The departure time of the first route is randomly generated between 8:00 and 9:30, and between 15:00 and 16:30 for the second. Similarly, the arrival time is randomly generated between 11:30 and 13:00 for the first route of each day, and between 18:30 and 20:00 for the second route of each day. The SOC consumption of each route is randomly generated between 0.4 and 0.47. The consideration of shorter routes should allow determining if it can be worthwhile to perform inter-route charging to keep degradation costs low by having more leeway regarding within which SOC intervals to cycle the battery at the expense of incurring peak or mid-peak energy costs.

5.1.1 Calibrating the charging infrastructure

We first solve the instances for the context with both day and night routes with a shorter planning horizon of two days while simultaneously optimizing the charging infrastructure in order to identify a reasonable charging infrastructure for subsequent tests. Since the instances with both day and night routes tend to consume more SOC during each day of the planning horizon, the charging infrastructures should be sufficient for the instances representing the other considered high use rate contexts as well. Also, since optimizing the charging infrastructure simultaneously makes the problem much harder to solve, the goal of these tests is not to reach near-exact solutions but simply to determine reasonable values for the number chargers to consider in our other experiments.

To this end, as suggested in Sassi and Oulamara (2014b), we define a fixed costs C_s representing the cost of acquiring and installing a charger of type s. We redefine parameter κ_s from the discrete time model as a non-negative integer variable, and add the term

$$\sum_{s \in S \setminus \{1\}} C_s \cdot \kappa_s$$

to the objective function, with $s = 1$ referring to the 2.5A charger which we assume comes with the vehicle when purchasing it. Lee et al. (2013) conclude that chargers allowing to fully charge electric trucks with 80kWh batteries between five and eight hours can cost up to \$15,000 including purchase costs and installation. Therefore, we consider purchase and installation costs of \$15,000 for the 7.5A (i.e., 5.3 hours full charge) charger, and \$30,000 (i.e., 2.7 hours full charge) for the 17.5A charger. Lee et al. (2013) also report an approximate lifetime of six years for such chargers. Assuming 260 working days per year, this yields fixed costs of approximately \$19 for the 7.5A charger and \$38 for the 17.5A charger in the context of a two day planning horizon. We solve the problem with the TOU-EV-4 plan with both summer and winter rates from Table 1, as well as with and without the degradation costs from Table 2.

The obtained charging infrastructures are reported in Tables 3 and 4, with S2 referring to the 7.5A charger and S3 refering to the 17.5A charger. Since the inclusion of degradation costs significantly increases total costs, both absolute and relative optimality gaps are reported. However, we reemphasize that the goal here is simply to determine a reasonable charging infrastructure for different fleet sizes and not to find near optimal solutions. Based on these results, a reasonable charging infrastructure for a fleet of m vehicles appears simply to be $\lceil \frac{m}{5} \rceil$ 17.5A chargers, which is the infrastructure we consider in the next sections whenever the TOU-EV-4 plan is used. This seems reasonable considering the fact that a company would most likely want to get by with only a few costly chargers.

Table 3: Best found charging infrastructures when minimizing energy and charger costs

	Summer rates				Winter rates			
Instance	Infrastructure	Time (s)	Abs. Gap (\$)	Rel. Gap (%)	Infrastructure	Time (s)	Abs. Gap (\$)	Rel. Gap (%)
1-5V	1XS3	4.98	0.36	0.29	1XS3	20.01	0.54	0.49
2-5V	1XS3	10.79	0.54	0.41	1XS3	66.92	0.49	0.42
3-5V	1XS3	7.83	0.54	0.43	1XS3	347.07	0.28	0.25
4-5V	1XS3	24.89	0.46	0.41	1XS3	19.92	0.06	0.07
5-5V	1XS3	37.38	0.53	0.46	1XS3	90.40	0.42	0.40
1-10V	2XS3	18000.00	20.41	8.56	1XS2+1XS3	18000.00	16.70	8.22
2-10V	2XS3	18000.00	21.70	9.28	1XS2+1XS3	18000.00	16.68	8.41
3-10V	1XS3	16543.90	0.95	0.47	1XS3	5706.21	0.83	0.48
4-10V	1XS2+1XS3	18000.00	13.01	5.99	1XS3	18000.00	0.97	0.55
5-10V	2XS3	18000.00	22.37	9.47	1XS2+1XS3	18000.00	16.80	8.39
1-15V	1XS2+2XS3	18000.00	20.42	6.18	1XS2+2XS3	18000.00	43.95	14.79
2-15V	3XS3	18000.00	23.13	6.39	3XS3	18000.00	55.81	17.02
3-15V	2XS3	10233.70	1.53	0.45	2XS3	18000.00	23.44	7.89
4-15V	1XS2+2XS3	18000.00	21.03	6.29	2XS3	18000.00	26.98	9.54
5-15V	3XS3	18000.00	24.56	6.60	1XS2+2XS3	18000.00	28.19	8.83

It is still interesting to note that for a given instance, regardless or whether degradation costs are considered, the infrastructure in the best found solution tends to be larger or faster when optimizing the problem using the summer rates, since energy costs are then larger

Table 4: Best found charging infrastructures when minimizing energy, charger and degradation costs

	Summer rates				Winter rates			
Instance	Infrastructure	Time (s)	Abs. Gap ($)	Rel. Gap (%)	Infrastructure	Time (s)	Abs. Gap ($)	Rel. Gap (%)
1-5V	1XS3	67.24	3.80	0.45	1XS3	15.23	3.30	0.40
2-5V	1XS3	66.17	3.45	0.37	1XS3	39.47	2.45	0.27
3-5V	1XS3	9.48	3.94	0.44	1XS3	4.98	3.58	0.41
4-5V	1XS3	5.95	3.70	0.48	1XS3	29.20	3.81	0.49
5-5V	1XS3	16.41	3.92	0.50	1XS3	2.71	3.15	0.41
1-10V	1XS2+1XS3	18000.00	18.23	1.08	2XS3	18000.00	18.05	1.10
2-10V	2XS3	439.43	7.45	0.46	1XS3	9484.99	7.34	0.47
3-10V	2XS3	16117.80	7.31	0.48	1XS3	14386.70	5.55	0.38
4-10V	2XS3	215.73	7.78	0.50	1XS3	3314.66	7.54	0.50
5-10V	2XS3	212.72	7.99	0.48	1XS3	4934.04	7.59	0.47
1-15V	3XS3	1385.09	11.74	0.50	1XS2+2XS3	18000.00	23.89	1.04
2-15V	1XS2+3XS3	18000.00	22.14	0.87	1XS2+3XS3	18000.00	56.45	2.25
3-15V	3XS3	16230.10	12.63	0.50	2XS2+2XS3	18000.00	41.44	1.65
4-15V	1XS2+3XS3	18000.00	21.02	0.88	1XS2+2XS3	18000.00	23.05	0.99
5-15V	3XS3	11092.80	9.17	0.35	2XS3	2391.48	12.35	0.49

during peak hours and lower during off-peak hours. Therefore, there is more incentive to have more or quicker chargers to do the bulk of the charging during specific periods of the day. This would suggest that the available time of use rates should be carefully considered when determining depot charging infrastructures.

5.1.2 Results under several scenarios

In this section we present results obtained under several scenarios with the charging infrastructure identified in the previous section. Results for the context with one day-time route and one night-time route are reported in Table 5. The average SOC column reports the average SOC of the vehicles upon departing for their routes. The figures show that total energy costs for the same instance tend to be higher with the summer rates than with the winter rates, regardless of whether degradation costs are considered or not. Indeed, the presence of night-time delivery routes takes away some of the best time periods (i.e., off-peak hours) to charge the vehicles in terms of energy costs, thereby forcing more charging to be done during mid-peak and peak hours during which energy costs are higher with the summer rates than the winter rates. Night-time delivery schemes incorporating EFVs may therefore be more appropriate during specific periods of the year. The figures also indicate that it may be worthwhile to incur slight increases in energy costs in order to decrease degradation costs by avoiding using the battery in the top 25% SOC interval.

The same holds for the scenario with each vehicle performing two short day-time delivery routes each day, presented in Table 6. However, in this case, the increase in energy costs

Table 5: Energy and degradation costs for instances with day-time and night-time routes

	Summer rates						Winter rates					
	Energy optimized			Energy and degradation optimized			Energy optimized			Energy and degradation optimized		
Instance	Energy costs	Deg. costs	Avg. SOC	Energy costs	Deg. costs	Avg. SOC	Energy costs	Deg. costs	Avg. SOC	Energy costs	Deg. costs	Avg. SOC
1-5V	125.35	1174.19	0.82	136.23	1091.90	0.72	108.87	1174.54	0.82	112.13	1094.45	0.73
2-5V	137.05	1238.10	0.82	144.96	1180.79	0.76	117.45	1231.91	0.81	119.51	1183.27	0.76
3-5V	136.42	1255.96	0.83	140.70	1198.48	0.77	117.93	1268.40	0.84	118.80	1200.87	0.77
4-5V	112.98	1059.33	0.76	120.95	994.92	0.68	99.61	1063.04	0.77	101.71	997.31	0.68
5-5V	129.37	1144.85	0.79	132.78	1094.95	0.73	110.61	1136.74	0.78	112.66	1094.03	0.72
1-10V	252.83	2385.39	0.84	262.10	2210.62	0.73	219.68	2344.93	0.82	224.54	2208.62	0.73
2-10V	251.55	2390.75	0.83	262.91	2234.67	0.73	220.06	2396.78	0.83	225.33	2239.08	0.74
3-10V	230.05	2188.93	0.78	240.22	2070.89	0.70	203.93	2228.80	0.80	212.09	2066.65	0.69
4-10V	243.67	2303.34	0.81	247.83	2158.55	0.71	213.67	2264.00	0.78	219.44	2156.80	0.71
5-10V	250.41	2337.30	0.81	259.04	2211.81	0.73	218.52	2371.97	0.82	223.22	2212.37	0.73
1-15V	357.45	3432.27	0.81	369.34	3196.71	0.71	315.51	3395.92	0.79	319.78	3200.80	0.71
2-15V	389.50	3673.00	0.84	403.73	3440.31	0.74	339.21	3635.85	0.82	344.84	3446.84	0.75
3-15V	379.48	3548.12	0.81	393.89	3354.18	0.73	331.68	3534.18	0.81	336.78	3361.71	0.74
4-15V	363.78	3486.57	0.82	381.93	3240.27	0.72	320.12	3480.87	0.81	327.76	3241.86	0.72
5-15V	384.18	3629.02	0.84	400.36	3380.01	0.73	334.36	3581.09	0.82	343.62	3384.37	0.74

between optimizing with and without degradation is more significant than in the day and night schemes. This is because in order to avoid cycling the battery in high SOC intervals and thereby keep degradation costs low, the only alternative is to perform more charging during peak hours between the two day routes. On the other hand, when optimizing solely energy costs in this context, in order to benefit from off-peak rates overnight, the vehicles regularly depart for the first route of the day with SOC values well above 0.9, thereby doing most of the charging overnight and keeping total energy costs much lower.

Table 6: Energy and degradation costs for instances with two short day-time routes

	Summer rates						Winter rates					
	Energy optimized			Energy and degradation optimized			Energy optimized			Energy and degradation optimized		
Instance	Energy costs	Deg. costs	Avg. SOC	Energy costs	Deg. costs	Avg. SOC	Energy costs	Deg. costs	Avg. SOC	Energy costs	Deg. costs	Avg. SOC
1-5V	54.39	729.89	0.70	102.01	656.93	0.61	55.32	734.38	0.70	77.59	603.02	0.50
2-5V	50.48	709.37	0.69	94.34	637.36	0.60	53.09	705.81	0.69	75.14	580.67	0.49
3-5V	53.38	721.52	0.70	98.63	646.86	0.61	54.46	718.68	0.70	76.85	591.39	0.50
4-5V	55.45	709.57	0.68	96.99	646.06	0.61	54.52	712.45	0.69	76.51	587.90	0.49
5-5V	51.55	716.89	0.70	99.86	642.69	0.60	53.89	716.27	0.70	75.05	592.44	0.51
1-10V	106.92	1447.97	0.70	193.58	1302.13	0.61	109.12	1439.81	0.69	152.51	1188.45	0.50
2-10V	107.43	1417.77	0.69	193.57	1279.63	0.60	108.01	1416.13	0.69	151.79	1170.03	0.49
3-10V	109.78	1465.31	0.70	205.34	1307.55	0.61	110.84	1460.26	0.70	155.48	1199.56	0.50
4-10V	105.63	1434.21	0.70	193.22	1283.68	0.61	108.10	1419.37	0.69	151.67	1174.15	0.50
5-10V	104.18	1449.64	0.70	202.33	1294.75	0.60	108.91	1451.57	0.69	154.06	1185.48	0.50
1-15V	158.59	2131.85	0.69	284.49	1917.31	0.60	161.68	2125.28	0.69	226.79	1751.22	0.49
2-15V	161.51	2170.07	0.70	299.62	1947.53	0.61	164.32	2168.29	0.69	230.22	1779.23	0.50
3-15V	164.23	2183.27	0.70	302.75	1961.12	0.61	165.60	2179.56	0.70	232.69	1790.41	0.50
4-15V	157.96	2150.20	0.69	300.16	1932.43	0.60	162.87	2154.96	0.70	229.45	1769.75	0.49
5-15V	160.35	2156.48	0.70	297.60	1942.29	0.61	163.39	2168.52	0.70	229.91	1775.38	0.50

Table 7 compares the results obtained when optimizing both energy and degradation costs with the two short day-time routes to a scenario within which the two short routes are merged into one single longer route. While performing one single longer route certainly has its logistical advantages, it also leaves much less leeway regarding which SOC intervals within which to cycle the battery and thus limits cycle aging mitigation. To generate the instances with one single long route per day, we simply merge the two routes of each vehicle into a single route, departing at the time of the earliest route, lasting the sum of the length of each route, and consuming the sum of the SOC consumption of each route. Therefore, in the single route per day scenario, all routes consume between 80% and 94% of the battery (note that 94% is the maximum feasible consumption for a route considering SOC_{min} and SOC_{max}). For the single long route scenario, the initial SOC of the vehicles is set to 0.8 in order to ensure feasibility, but the energy and degradation costs are adjusted (assuming only off-peak rates for the energy costs) in order to draw comparisons to the results with the two shorter day-time routes (for which the initial SOC of the vehicles is 0.5).

The results indicate that even in presence of cheap overnight electricity costs, when degradation costs are jointly minimized, in terms of total costs it becomes preferable to split the long route into two parts and incur peak energy rates in order to avoid cycling the battery in high SOC intervals, rather than benefit more from off-peak rates but be limited with regards to cycle aging mitigation. Moreover, the two short day-time routes context in Tables 6 and 7 is somewhat a worst case scenario, since almost all the time available for charging between the two routes occurs during peak hours.

Table 7: Cost comparison of two short routes with one long route

	Summer rates								Winter rates							
	One long route				Two short routes				One long route				Two short routes			
Instance	Energy costs	Deg. costs	Avg. SOC	Total	Energy costs	Deg. costs	Avg. SOC	Total	Energy costs	Deg. costs	Avg. SOC	Total	Energy costs	Deg. costs	Avg. SOC	Total
1-5V	45.92	742.58	0.93	788.50	102.01	656.93	0.61	758.94	52.77	742.99	0.93	795.76	77.59	603.02	0.50	680.61
2-5V	45.54	712.06	0.91	757.60	94.34	637.36	0.60	731.70	51.21	712.06	0.91	763.27	75.14	580.67	0.49	655.81
3-5V	44.88	728.17	0.92	773.05	98.63	646.86	0.61	745.49	52.32	729.43	0.92	781.75	76.85	591.39	0.50	668.24
4-5V	43.04	724.27	0.92	767.31	96.99	646.06	0.61	743.05	52.97	725.67	0.92	778.64	76.51	587.90	0.49	664.41
5-5V	44.11	724.60	0.92	768.71	99.86	642.69	0.60	742.55	51.70	724.64	0.92	776.34	75.05	592.44	0.51	667.49
1-10V	93.10	1458.14	0.92	1551.24	193.58	1302.13	0.61	1495.71	108.44	1459.35	0.92	1567.79	152.51	1188.45	0.50	1340.96
2-10V	89.30	1439.02	0.91	1528.32	193.57	1279.63	0.60	1472.20	105.99	1438.08	0.91	1544.07	151.79	1170.03	0.49	1321.82
3-10V	89.39	1479.94	0.93	1569.33	205.34	1307.55	0.61	1512.89	106.26	1480.07	0.93	1586.33	155.48	1199.56	0.50	1355.04
4-10V	86.35	1441.57	0.91	1527.92	193.22	1283.68	0.61	1475.90	104.94	1442.78	0.92	1547.72	151.67	1174.15	0.50	1325.82
5-10V	89.05	1464.75	0.92	1553.80	202.33	1294.75	0.60	1497.08	109.48	1462.63	0.92	1572.11	154.06	1185.48	0.50	1339.54
1-15V	134.21	2148.61	0.91	2282.82	284.49	1917.31	0.60	2201.80	157.42	2149.33	0.91	2306.75	226.79	1751.22	0.49	1978.01
2-15V	136.94	2194.73	0.92	2331.67	299.62	1947.53	0.61	2247.15	160.77	2196.80	0.92	2357.57	230.22	1779.23	0.50	2009.45
3-15V	137.55	2209.44	0.93	2346.99	302.75	1961.12	0.61	2263.87	164.08	2209.44	0.93	2373.52	232.69	1790.41	0.50	2023.10
4-15V	134.36	2180.49	0.92	2314.85	300.16	1932.43	0.60	2232.59	164.36	2176.71	0.92	2341.07	229.45	1769.75	0.49	1999.20
5-15V	131.67	2190.07	0.92	2321.74	297.60	1942.29	0.61	2239.89	157.84	2184.94	0.92	2342.78	229.91	1775.38	0.50	2005.29

A better context for mitigating both energy and degradation costs would therefore most likely be to have two short day-time routes allowing intermittent charging during mid-peak hours or off-peak hours. To assess whether this scenario could generate significant savings, we first modified the instances with two short day-time routes by shifting the second route of each day by four hours, thereby departing between 19:00 and 20:30. Table 8 compares the results obtained when optimizing both energy and degradation costs with the single long route and with the two short routes further apart from each other. The figures indicate that the delaying the second routes to the evening allows reducing both energy and degradation costs compared to the scenario with the two routes closer to each other, especially with the summer rates, during which peak rates are much higher. Indeed, with the summer rates, inter-route charging is delayed to the few hours of mid-peak rates prior to the second route for as many vehicles as possible.

Finally, we also solved the instances with the larger delay between the routes while simultaneously shifting all routes of half the fleet five hours later, thereby allowing half the fleet to perform their first route in the early afternoon hours and their second route in the early portions of the night. The results are reported in Table 9 and show that energy and degradation costs are further reduced, thereby indicating that this scenario constitutes the best alternative to the single long daily route. Indeed, in this case, the SOC of the vehicles is kept even lower and almost all inter-route charging is done outside peak hours.

Table 8: Cost comparison of two short routes further apart from each other with one long route

	Summer rates								Winter rates							
	One long route				Two short routes further apart				One long route				Two short routes further apart			
Instance	Energy costs	Deg. costs	Avg. SOC	Total	Energy costs	Deg. costs	Avg. SOC	Total	Energy costs	Deg. costs	Avg. SOC	Total	Energy costs	Deg. costs	Avg. SOC	Total
1-5V	45.92	742.58	0.93	788.50	69.05	649.01	0.59	718.06	52.77	742.99	0.93	795.76	73.41	600.79	0.50	674.20
2-5V	45.54	712.06	0.91	757.60	65.94	618.01	0.56	683.95	51.21	712.06	0.91	763.27	70.20	578.60	0.49	648.80
3-5V	44.88	728.17	0.92	773.05	67.34	631.02	0.58	698.36	52.32	729.43	0.92	781.75	71.95	590.61	0.49	662.56
4-5V	43.04	724.27	0.92	767.31	67.31	628.30	0.57	695.61	52.97	725.67	0.92	778.64	71.74	585.60	0.49	657.34
5-5V	44.11	724.60	0.92	768.71	67.43	636.03	0.59	703.46	51.70	724.64	0.92	776.34	72.41	585.90	0.49	658.31
1-10V	93.10	1458.14	0.92	1551.24	137.09	1269.03	0.58	1406.12	108.44	1459.35	0.92	1567.79	143.72	1182.53	0.49	1326.25
2-10V	89.30	1439.02	0.91	1528.32	134.70	1244.09	0.57	1378.79	105.99	1438.08	0.91	1544.07	142.12	1168.35	0.49	1310.47
3-10V	89.39	1479.94	0.93	1569.33	139.42	1272.81	0.57	1412.23	106.26	1480.07	0.93	1586.33	144.72	1194.71	0.50	1339.43
4-10V	86.35	1441.57	0.91	1527.92	133.54	1255.05	0.58	1388.59	104.94	1442.78	0.92	1547.72	141.72	1171.68	0.49	1313.40
5-10V	89.05	1464.75	0.92	1553.80	142.97	1257.11	0.57	1400.08	109.48	1462.63	0.92	1572.11	142.30	1185.84	0.50	1328.14
1-15V	134.21	2148.61	0.91	2282.82	196.99	1872.98	0.57	2201.80	157.42	2149.33	0.91	2306.75	213.35	1745.58	0.49	1978.01
2-15V	136.94	2194.73	0.92	2331.67	208.66	1888.61	0.57	2097.27	160.77	2196.80	0.92	2357.57	214.67	1777.78	0.49	1992.45
3-15V	137.55	2209.44	0.93	2346.99	213.34	1908.67	0.58	2122.01	164.08	2209.44	0.93	2373.52	217.76	1787.60	0.50	2005.36
4-15V	134.36	2180.49	0.92	2314.85	206.64	1881.25	0.57	2087.89	164.36	2176.71	0.92	2341.07	212.28	1768.89	0.49	1981.17
5-15V	131.67	2190.07	0.92	2321.74	206.95	1892.76	0.57	2099.71	157.84	2184.94	0.92	2342.78	215.10	1767.53	0.49	1982.63

5.2 The impact of grid restrictions

We now investigate the impact of maximum allowed loads on energy and degradation costs by considering another rate plan offered by Southern California Edison (2017): TOU-EV-3-A. Under this plan, the maximum power retrieved from the grid must always remain below 20kW. We therefore limit ourselves to a fleet size of five vehicles. Since the 17.5A charger alone surpasses the maximum allowable charging power, we also consider a different charging infrastructure. We assume five 2.5A chargers, two 5A charger, and one 7.5A charger. The 5A charger is capable of charging the battery from SOC_{min} to SOC_{max} in approximately 7.9 hours and uses a charging power of approximately 10kW. The CV process is entered at

Table 9: Cost comparison of two short routes further apart from each other and less clustered with one long route

	Summer rates								Winter rates							
	One long route				Two short routes further apart and less clustered				One long route				Two short routes further apart and less clustered			
Instance	Energy costs	Deg. costs	Avg. SOC	Total	Energy costs	Deg. costs	Avg. SOC	Total	Energy costs	Deg. costs	Avg. SOC	Total	Energy costs	Deg. costs	Avg. SOC	Total
1-5V	45.92	742.58	0.93	788.50	66.06	617.08	0.54	683.14	52.77	742.99	0.93	795.76	65.43	599.90	0.50	665.33
2-5V	45.54	712.06	0.91	757.60	61.39	588.81	0.51	650.20	51.21	712.06	0.91	763.27	62.19	579.22	0.49	641.41
3-5V	44.88	728.17	0.92	773.05	60.23	603.35	0.52	663.58	52.32	729.43	0.92	781.75	63.07	589.57	0.49	652.64
4-5V	43.04	724.27	0.92	767.31	61.25	598.50	0.51	659.75	52.97	725.67	0.92	778.64	62.25	587.08	0.49	649.33
5-5V	44.11	724.60	0.92	768.71	60.48	608.05	0.53	668.53	51.70	724.64	0.92	776.34	64.34	585.48	0.49	649.82
1-10V	93.10	1458.14	0.92	1551.24	123.98	1196.96	0.51	1320.94	108.44	1459.35	0.92	1567.79	123.67	1180.48	0.49	1304.15
2-10V	89.30	1439.02	0.91	1528.32	121.47	1177.17	0.50	1298.64	105.99	1438.08	0.91	1544.07	121.01	1168.20	0.49	1289.21
3-10V	89.39	1479.94	0.93	1569.33	125.47	1205.11	0.51	1330.58	106.26	1480.07	0.93	1586.33	125.09	1193.98	0.50	1319.07
4-10V	86.35	1441.57	0.91	1527.92	120.08	1191.60	0.51	1311.68	104.94	1442.78	0.92	1547.72	123.31	1166.98	0.49	1290.29
5-10V	89.05	1464.75	0.92	1553.80	124.55	1191.19	0.50	1315.74	109.48	1462.63	0.92	1572.11	124.03	1183.96	0.49	1307.99
1-15V	134.21	2148.61	0.91	2282.82	180.55	1771.70	0.51	1952.25	157.42	2149.33	0.91	2306.75	181.79	1748.02	0.49	1929.81
2-15V	136.94	2194.73	0.92	2331.67	183.92	1796.14	0.51	1980.06	160.77	2196.80	0.92	2357.57	184.35	1774.55	0.49	1958.90
3-15V	137.55	2209.44	0.93	2346.99	184.70	1822.39	0.52	2007.09	164.08	2209.44	0.93	2373.52	188.46	1788.72	0.50	1977.18
4-15V	134.36	2180.49	0.92	2314.85	182.91	1790.86	0.51	1973.77	164.36	2176.71	0.92	2341.07	185.22	1757.56	0.49	1942.78
5-15V	131.67	2190.07	0.92	2321.74	181.56	1808.92	0.52	1990.48	157.84	2184.94	0.92	2342.78	187.27	1770.80	0.49	1958.07

a SOC of 0.97 after approximately 7.4 hours, so we approximate the CC-CV process with two SOC breakpoints: 0.05, 0.97, and 0.99. The charging currents used in our piecewise approximation for this charger are 5A between 0.05 and 0.97, and 1.6A between 0.97 and 0.99. To ensure that no instances would be infeasible due to the initial SOC of the vehicles, we set this parameter to 0.99.

All instances with five vehicles for the day and night routes scenario become infeasible with the grid restriction and the new charging infrastructure. When removing the grid constraints, these instances become feasible with the charging infrastructure. One of the instances with five vehicles for the single long day-time route also became infeasible with the grid restriction and feasible when removing it. This suggests that such grid restrictions can indeed hinder high EFV utilization in contexts with relatively long routes.

We also solved the instances with two shorter routes per day and the same variations from the previous section but with the new charging infrastructure, as well as with and without the grid restriction of 20kW. The results are reported in Table 10, in which G refers to the presence of the grid restriction and NG refers to no grid restriction during the optimization process. The number preceding G or NG indicates the scenario considered: 1 refers to the initial considered scenario with two day-time routes; 2 refers to the two routes with an additional four hours between the first and second route of each day; and 3 refers to the two routes with an additional four hours between the first and second route of each day and with half the fleet's routes shifted five hours later.

The model still manages to reduce degradation costs significantly when the grid restriction is in place, at the expense of higher energy costs. The most notable impact of the grid restriction is on energy costs. With the summer rates, energy costs are sometimes nearly

Table 10: The impact of grid restrictions on energy and degradation costs

	Summer rates				Winter rates			
	Energy optimized		Energy and degradation optimized		Energy optimized		Energy and degradation optimized	
Instance	Energy costs	Deg. costs	Energy costs	Deg. costs	Energy costs	Deg. costs	Energy costs	Deg. costs
1-5V-1-G	110.65	554.61	115.14	514.41	83.53	557.51	84.00	514.56
2-5V-1-G	100.57	531.39	110.18	487.61	79.35	551.54	80.59	485.75
3-5V-1-G	108.13	542.64	115.28	495.61	81.83	543.23	82.33	495.67
4-5V-1-G	104.68	539.53	113.07	492.41	80.94	530.28	82.00	492.64
5-5V-1-G	104.03	544.94	109.63	498.62	80.86	553.87	81.21	498.90
1-5V-1-NG	61.48	569.61	105.05	506.18	68.34	569.30	85.39	479.79
2-5V-1-NG	58.82	543.06	96.06	488.03	65.46	548.05	82.77	458.13
3-5V-1-NG	60.37	553.55	97.62	498.16	67.06	554.34	84.62	465.33
4-5V-1-NG	59.83	546.49	95.34	498.04	66.53	547.75	84.81	460.44
5-5V-1-NG	59.69	552.40	97.25	495.07	66.32	552.49	81.44	471.06
1-5V-2-G	122.05	554.46	130.37	480.10	84.71	560.78	86.18	478.84
2-5V-2-G	107.70	551.62	120.39	460.06	80.17	543.07	83.22	452.59
3-5V-2-G	116.53	542.65	126.42	467.49	82.99	552.68	84.92	461.90
4-5V-2-G	112.40	538.97	124.50	464.67	81.94	539.60	83.99	459.41
5-5V-2-G	116.85	548.04	124.32	468.31	81.91	553.25	83.38	464.25
1-5V-2-NG	61.34	567.55	79.74	506.29	68.44	563.61	86.82	465.34
2-5V-2-NG	58.98	541.53	72.48	486.34	65.57	544.31	83.53	447.12
3-5V-2-NG	60.12	553.54	78.52	491.74	67.08	550.48	84.91	455.86
4-5V-2-NG	60.05	545.78	75.53	489.38	66.48	547.03	83.65	454.64
5-5V-2-NG	59.75	553.37	72.55	497.33	66.35	553.37	84.41	452.50
1-5V-3-G	84.87	558.57	105.69	472.94	79.91	551.35	83.86	467.07
2-5V-3-G	80.71	532.47	93.77	459.19	76.30	533.12	81.33	447.30
3-5V-3-G	82.42	545.60	102.74	461.05	77.93	545.60	82.34	456.90
4-5V-3-G	81.42	524.94	100.61	460.88	77.47	533.84	81.26	453.11
5-5V-3-G	81.69	545.26	102.59	460.92	77.29	537.68	81.87	453.23
1-5V-3-NG	61.95	567.43	80.61	482.86	68.61	566.25	82.13	466.17
2-5V-3-NG	58.99	551.14	73.43	465.40	65.43	554.06	78.49	445.81
3-5V-3-NG	60.12	554.60	74.41	475.22	66.80	554.60	79.85	455.18
4-5V-3-NG	59.86	534.80	73.03	472.53	66.56	535.66	79.09	452.77
5-5V-3-NG	59.71	548.37	73.30	477.37	66.64	544.65	79.66	453.16

doubled when solving the same instance without the grid restriction and with the grid restriction of 20kW. Indeed, the grid restriction prevents the model from taking advantage of significant savings regarding energy costs since it limits the number of vehicles that can be simultaneously charged at any given moment (e.g., when energy is cheaper). The increase in energy costs is, however, less significant with the winter rates, since energy costs outside off-peak hours are smaller. Regardless of the seasonal rate and whether energy costs are minimized alone or jointly with the degradation costs, the best scenario with the grid restriction is the one in which the two routes of each day are further apart from each other and less clustered (i.e., with half the fleet's route shifted five hours later).

5.3 The impact of facilities related demand charges

Our numerical experiments have so far disregarded FRD charges that are present in rate plans TOU-EV-4 and TOU-EV-3B form Table 1. To investigate whether optimizing charging schedules while ignoring such charges may lead to undesirable solutions, we solved some of the previous test instances while jointly optimizing the FRD charge. To incorporate this into the problem, we added the following constraints to the discrete time model:

$$\sum_{k \in K} \sum_{s \in S} \sum_{i \in B_s \setminus \{0\}} x_{pksi} \cdot P_s \leq F \qquad p \in P \tag{70}$$

and we changed the objective function to

$$\text{minimize} \quad \sum_{k \in K} \sum_{p \in P} \frac{i_{pk} \cdot \delta}{Q} \cdot QE \cdot c_p + \sum_{r \in R} \sum_{d \in D} QE \cdot \Delta soc_{dr} \cdot W_d + F \cdot c_{FRD}, \tag{71}$$

where F is a decision variable indicating the maximum charging power retrieved from the grid over the planning horizon, and c_{FRD} is the FRD charge under the considered rate plan.

We first solved the instances with relatively long day and night routes as well as the instances with two short routes per day (under the best scenario, i.e., with routes far apart and less clustered) with energy costs, degradation costs and the FRD charge under plan TOU-EV-4. The monthly FRD charge under this plan is $13.20/kW. Assuming 22 working days per month, this would be equivalent to an FRD charge of $1.8/kW over a planning horizon of three days. Since the initial SOC of the vehicles in these instances is set to 0.5, we only start applying the FRD charge several hours after the start of the horizon to allow the vehicles to reach an appropriate SOC for their first route without incurring the FRD fee.

The joint optimization of the FRD charge makes the problem significantly harder to solve, and the solver was unable to find a solution with an optimality gap under 0.5% for only a few of these instances. For two of the instances with day and night routes, the solver was unable to find an integer solution within the time limit, and for three other instances, the best found solution had an optimality gap between 0.5% and 0.7%. For four of the instances with two shorter routes per day, the best found solution had an optimality gap between 0.5% and 1.4%. The results are reported in Tables 11 and 12.

Table 11: Day-time and night-time routes: the impact of FRD charges on costs

	Summer rates						Winter rates					
	Optimized with FRD charge			Optimized without FRD charge			Optimized with FRD charge			Optimized without FRD charge		
Instance	Energy costs	Deg. costs	FRD charge	Energy costs	Deg. costs	FRD charge	Energy costs	Deg. costs	FRD charge	Energy costs	Deg. costs	FRD charge
1-5V	141.61	1094.09	81.00	136.23	1091.90	99.00	116.35	1094.60	72.00	112.13	1094.45	99.00
2-5V	150.28	1186.43	81.00	144.96	1180.79	99.00	121.44	1182.60	81.00	119.51	1183.27	99.00
3-5V	147.68	1195.96	81.00	140.70	1198.48	99.00	124.69	1194.97	72.00	118.80	1200.87	99.00
4-5V	126.83	995.85	81.00	120.95	994.92	99.00	104.79	994.47	72.00	101.71	997.31	99.00
5-5V	143.63	1096.20	81.00	132.78	1094.95	99.00	116.09	1097.05	72.00	112.66	1094.03	99.00
1-10V	280.50	2208.41	162.00	262.10	2210.62	198.00	229.21	2201.85	144.00	224.54	2208.62	198.00
2-10V	270.79	2236.77	162.00	262.91	2234.67	198.00	230.64	2231.49	144.00	225.33	2239.08	198.00
3-10V	248.97	2068.84	162.00	240.22	2070.89	198.00	218.67	2062.49	135.00	212.09	2066.65	198.00
4-10V	256.18	2158.38	162.00	247.83	2158.55	198.00	226.18	2155.01	135.00	219.44	2156.80	198.00
5-10V	265.75	2212.31	162.00	259.04	2211.81	198.00	233.35	2206.72	135.00	223.22	2212.37	198.00
1-15V	392.02	3202.97	225.00	369.34	3196.71	297.00	331.24	3188.84	207.00	319.78	3200.80	297.00
2-15V	411.39	3440.71	252.00	403.73	3440.31	297.00	-	-	-	344.84	3446.84	297.00
3-15V	405.58	3356.61	243.00	393.89	3354.18	297.00	346.51	3349.56	207.00	336.78	3361.71	297.00
4-15V	-	-	-	381.93	3240.27	297.00	341.86	3240.72	207.00	327.76	3241.86	297.00
5-15V	421.24	3383.63	243.00	400.36	3380.01	297.00	349.19	3377.56	216.00	343.62	3384.37	288.00

Table 12: Two short routes far apart and declustered: the impact of FRD charges on costs

	Summer rates						Winter rates					
	Optimized with FRD charge			Optimized without FRD charge			Optimized with FRD charge			Optimized without FRD charge		
Instance	Energy costs	Deg. costs	FRD charge	Energy costs	Deg. costs	FRD charge	Energy costs	Deg. costs	FRD charge	Energy costs	Deg. costs	FRD charge
1-5V	61.43	627.56	63.00	66.06	617.08	81.00	74.41	603.82	36.00	65.43	599.90	81.00
2-5V	59.60	595.51	63.00	61.39	588.81	81.00	71.62	579.98	36.00	62.19	579.22	81.00
3-5V	60.02	608.10	63.00	60.23	603.35	81.00	73.19	591.39	36.00	63.07	589.57	81.00
4-5V	58.39	607.50	63.00	61.25	598.50	90.00	72.72	588.66	36.00	62.25	587.08	81.00
5-5V	62.09	613.03	63.00	60.48	608.05	81.00	72.22	590.50	36.00	64.34	585.48	81.00
1-10V	161.49	1206.71	81.00	123.98	1196.96	153.00	141.90	1178.90	63.00	123.67	1180.48	153.00
2-10V	159.23	1189.01	81.00	121.47	1177.17	171.00	140.16	1164.41	63.00	121.01	1168.20	153.00
3-10V	164.92	1212.77	81.00	125.47	1205.11	153.00	143.85	1194.07	63.00	125.09	1193.98	153.00
4-10V	156.40	1190.85	90.00	120.08	1191.60	153.00	139.71	1168.45	63.00	123.31	1166.98	153.00
5-10V	157.37	1200.96	90.00	124.55	1191.19	153.00	142.66	1180.97	63.00	124.03	1183.96	153.00
1-15V	238.82	1767.50	135.00	180.55	1771.70	234.00	196.98	1738.22	126.00	181.79	1748.02	234.00
2-15V	226.19	1805.93	144.00	183.92	1796.14	234.00	201.19	1768.76	126.00	184.35	1774.55	234.00
3-15V	238.00	1816.49	144.00	184.70	1822.39	234.00	213.51	1779.32	99.00	188.46	1788.72	234.00
4-15V	228.63	1791.48	144.00	182.91	1790.86	234.00	199.21	1757.24	126.00	185.22	1757.56	234.00
5-15V	249.85	1798.31	135.00	181.56	1808.92	234.00	201.97	1762.72	126.00	187.27	1770.8	234.00

The figures of Tables 11 and 12 deserve some comments. First, the FRD charge is higher when solving a given instance with the summer rates than with the winter rates. For the instances with two shorter routes, this outcome is a consequence of the necessity to charge the vehicles between their routes to keep departing SOC values and thus degradation costs low. With the winter rates, energy costs during peak hours are sufficiently low for it to be beneficial to charge vehicles a little bit during peak hours and thus keep FRD charges low by spreading out the inter-route charging of vehicles over larger time intervals. On the other hand, with the summer rates, the model waits until mid-peak hours to perform inter-route charging in order to avoid very high peak rates, thereby requiring one to charge more vehicles within a shorter time interval or to use faster chargers retrieving more power from the grid, thus incurring higher FRD charges. A similar phenomenon is identified in the day and night route instances. When a vehicle returns from its day-time route before 18:00 with the winter rates, it tends to start being charged as soon as possible despite peak rates still being in place. With the summer rates, the charging of those vehicles prior to their night-time route is usually postponed to mid-peak hours or off-peak hours.

Second, the results suggest that optimizing the charging schedule without considering the FRD charges may lead to solutions in which the decrease in energy costs does not make up for the higher FRD charge. Indeed, in several of the instances, the reduction in the FRD fee obtained by jointly optimizing energy, FRD and degradation costs outweighs the increase in energy costs resulting from having to spread out charging events to more costly periods of the day, while still generating similar degradation costs. All in all, the results suggest that disregarding FRD fees when optimizing the charging schedule may lead to solutions with FRD fees that do not justify the corresponding savings in energy costs.

To assess the impact of degradation costs on FRD charges, we also solved the instances with two shorter routes by optimizing the charging schedule with energy and FRD costs but without the degradation costs. Here again, some instances returned optimality gaps above 0.5% after the five hour time limit, with a value of 3.22% in the worst case. Table 13 compares the results of this experiment to those obtained when energy, FRD and degradation costs are simultaneously optimized. The results suggest that incurring larger FRD fees can be well worthwhile in order to lower degradation costs.

Finally, as already mentioned, two options are available for the TOU-EV-3 rate plan (see Table 1). Option A has higher energy costs but no FRD charge, while option B has lower energy costs but an FRD charge. Both are subject to the maximum charging power of 20kW. In order to show how the model may be used to choose among different rate plans in such contexts, we solved the instances with two short routes with a fleet of five vehicles and the charging infrastructure of Section 5.2 (because of the 20kW grid restriction) with both TOU-EV-3 plan options, as well as with and without degradation costs. In this case, the \$7.23/kW monthly FRD fee is equivalent to approximately \$0.99/kW for the three day

Table 13: The cost impact of degradation costs on FRD charges

	Summer rates						Winter rates					
	Energy, deg. and FRD optimized			Energy and FRD optimized			Energy, deg. and FRD optimized			Energy and FRD optimized		
Instance	Energy costs	Deg. costs	FRD charge	Energy costs	Deg. costs	FRD charge	Energy costs	Deg. costs	FRD charge	Energy costs	Deg. costs	FRD charge
1-5V	61.43	627.56	63.00	51.22	697.18	63.00	74.41	603.82	36.00	70.51	723.52	27.00
2-5V	59.60	595.51	63.00	48.70	678.33	63.00	71.62	579.98	36.00	67.78	707.51	27.00
3-5V	60.02	608.10	63.00	49.48	679.35	63.00	73.19	591.39	36.00	69.33	683.83	27.00
4-5V	58.39	607.50	63.00	48.86	664.64	63.00	72.72	588.66	36.00	68.82	695.08	27.00
5-5V	62.09	613.03	63.00	49.07	683.06	63.00	72.22	590.50	36.00	68.41	704.92	27.00
1-10V	161.49	1206.71	81.00	144.70	1364.48	63.00	141.90	1178.90	63.00	141.33	1418.97	45.00
2-10V	159.23	1189.01	81.00	134.95	1338.71	72.00	140.16	1164.41	63.00	138.60	1395.40	45.00
3-10V	164.92	1212.77	81.00	146.56	1359.00	63.00	143.85	1194.07	63.00	143.90	1431.05	45.00
4-10V	156.40	1190.85	90.00	135.33	1346.95	72.00	139.71	1168.45	63.00	139.73	1426.55	45.00
5-10V	157.37	1200.96	90.00	137.81	1379.60	72.00	142.66	1180.97	63.00	142.52	1410.87	45.00
1-15V	238.82	1767.50	135.00	187.37	1970.71	126.00	196.98	1738.22	126.00	203.48	2055.62	72.00
2-15V	226.19	1805.93	144.00	193.68	2017.09	126.00	201.19	1768.76	126.00	207.87	2110.92	72.00
3-15V	238.00	1816.49	144.00	194.19	2058.27	126.00	213.51	1779.32	99.00	209.33	2108.41	72.00
4-15V	228.63	1791.48	144.00	190.71	2035.51	126.00	199.21	1757.24	126.00	206.35	2085.46	72.00
5-15V	249.85	1798.31	135.00	193.76	2025.95	126.00	201.97	1762.72	126.00	201.26	2108.30	81.00

planning horizon, assuming once again 22 working days per month. The results are reported in Table 14. A solution with an optimality gap below 0.5% was found for all instances. In this case, whether degradation costs are jointly optimized or not, both plan options appear to be equivalent in terms of total cost, i.e., the savings in energy costs with the TOU-EV-3-B plan are approximately equivalent to the additional FRD fee. Nevertheless, this experiment demonstrates how the model can be used to compare different plan options when such alternatives are availalable. Moreover, note that in all solutions with an FRD charge of $14.85 (corresponding to a maximum charging power of 15kW over the planning horizon) in Table 14, the two 5A-10kW chargers are never used simultaneously, while this is not the case in solutions obtained when the same instance is solved with the rate plan offering higher energy rates but no FRD charge. The same total cost can thus sometimes be obtained by using a smaller charging infrastructure with the plan including the FRD charge.

Table 14: Cost comparison of the TOU-EV-3 plan options

	Summer rates							Winter rates						
	Energy and FRD optimized			Energy, FRD and degradation optimized				Energy and FRD optimized			Energy, FRD and degradation optimized			
Instance	Energy costs	FRD charge	Total	Energy costs	FRD charge	Deg. costs	Total	Energy costs	FRD charge	Total	Energy costs	FRD charge	Deg. costs	Total
1-5V-TOU-EV-3-A	84.87	0.00	84.87	105.69	0.00	472.94	578.63	79.91	0.00	79.91	83.86	0.00	467.07	550.93
2-5V-TOU-EV-3-A	80.71	0.00	80.71	93.77	0.00	459.19	552.96	76.30	0.00	76.30	81.33	0.00	447.30	528.63
3-5V-TOU-EV-3-A	82.42	0.00	82.42	102.74	0.00	461.05	563.79	77.93	0.00	77.93	82.34	0.00	456.90	539.24
4-5V-TOU-EV-3-A	81.42	0.00	81.42	100.61	0.00	460.88	561.49	77.47	0.00	77.47	81.26	0.00	453.11	534.37
5-5V-TOU-EV-3-A	81.69	0.00	81.69	102.59	0.00	460.92	563.51	77.29	0.00	77.29	81.87	0.00	453.23	535.10
1-5V-TOU-EV-3-B	64.30	19.80	84.10	84.52	19.80	473.57	577.89	63.79	14.85	78.64	62.60	19.80	465.34	547.74
2-5V-TOU-EV-3-B	61.10	19.80	80.90	74.99	19.80	458.33	553.12	60.79	14.85	75.64	62.31	14.85	448.29	525.45
3-5V-TOU-EV-3-B	62.66	19.80	82.46	80.58	19.80	462.83	563.21	62.10	14.85	76.95	63.69	14.85	457.68	536.22
4-5V-TOU-EV-3-B	61.73	19.80	81.53	85.59	19.80	455.33	560.72	61.46	14.85	76.31	63.10	14.85	454.84	532.79
5-5V-TOU-EV-3-B	61.85	19.80	81.65	82.36	19.80	461.60	563.76	61.79	14.85	76.64	63.09	14.85	454.16	532.10

5.4 Calendar aging considerations

Degradation occuring while the battery is stored is always worse at high SOC values. Lunz et al. (2012) showed that significant lifetime savings can be attained by charging electric vehicles as closely as possible to their departure times in order to avoid spending lengthy periods of time in higher SOC values. Alghough there exist some calendar aging models translating storage degradation in monetary terms, these rely on extensive long-term experimental data (e.g., Hoke et al. 2011) that may not be readily available for any given battery. Nevertheless, it would be desirable to at least mitigate calendar aging when this can be achieved without affecting the quality of the solution obtained without calendar aging considerations.

A significant benefit of the non-decreasing wear function used in all previous experiments is that cycling the battery in lower SOC intervals not only increases cycle life, but also indirectly helps calendar life. This is, however, not the case when the battery wear function is non-increasing. Indeed, the cycle life data of some batteries may result in non-increasing cycling wear functions, meaning that it would be preferable to avoid cycling such batteries in low SOC values. This would most likely lead to an increase in calendar aging. We illustrate this by solving the instances with two short delivery routes (further apart from each other and declustered) with the DOD cycle life data used in Hoke et al. (2011), which results in the non-increasing wear function reported in Table 15 (note that this battery has a higher cycle life than the one previously considered and thus lower wear costs).

Table 15: Non-increasing battery degradation costs

SOC interval	Degradation costs
0-0.25	\$0.57/kWh
0.25-0.5	\$0.49/kWh
0.5-0.75	\$0.38/kWh
0.75-1	\$0.22/kWh

The results are reported in Table 16 with the winter rates of the TOU-EV-4 plan. The cycle life of the vehicles is estimated by assuming the operating conditions over the planning horizon of three days would be repeated until cumulative degradation costs reach the battery price. The calendar life is estimated by weighing the calendar lifetime of SOC intervals of 10% with the frequency of occurence of these SOC intervals in the solution, as in Lunz et al. (2012). The calendar lifetime of each SOC interval is extrapolated from accelerated calendar aging tests for electric vehicle lithium-ion cells reported in Lunz et al. (2012). In the determination of the calendar life of the batteries, it is assumed that their SOC decreases linearly from period to period while they performs routes. The column “Avg. Cal. Life NDWF ”reports the average estimated calendar life obtained for the same instance when optimizing energy and degradation costs with the non-decreasing wear costs used in all previous experiments. The average SOC column reports the average SOC of the vehicles upon departing for their routes.

The results presented in Table 16 show that calendar life is adversely affected when optimizing the charging schedule with the non-increasing battery wear function. For each instance, optimizing without the degradation costs yields solutions in which the average estimated cycle life of the batteries is lower than the average estimated calendar life. On the other hand, optimizing with the degradation costs increases the average cycle life of the batteries, but significantly lowers the average calendar life, since the batteries spend much more time in high SOC intervals. The estimated average calendar life actually falls below the cycle life when energy and degradation are jointly optimized with the degradation costs from Table 15, naturally leading one to question whether the cycle life savings and associated increase in energy costs are really worthwhile. One should therefore carefully use such wear functions and ensure that the savings in cycle life outweigh the loss of calendar life and increase in energy costs.

The results also clearly demonstrate the calendar aging benefit of the non-decreasing battery wear function from Table 2, since jointly optimizing degradation and energy costs is beneficial to both cycle life (as demonstrated in our previous experiments through the reduction of degradation costs) and calendar life, which increases for each instance in Table 16 (see column "Avg. Cal. Life NDWF ") compared to the solution obtained when only energy costs are minimized.

Table 16: Adverse impact of non-increasing battery degradation costs on calendar life

	Energy optimized					Energy and degradation optimized					
Instance	Energy costs	Deg. costs	Avg. SOC	Avg. Cyc. Life	Avg. Cal. Life	Energy costs	Deg. costs	Avg. SOC	Avg. Cyc. Life	Avg. Cal. Life	Avg. Cal. Life NDWF
1-5V	53.42	383.18	0.66	5.82	8.55	66.60	263.75	0.89	7.73	6.82	9.92
2-5V	51.34	364.22	0.66	6.05	8.48	63.08	253.72	0.89	7.95	6.80	10.07
3-5V	52.34	378.49	0.65	5.88	8.64	64.65	263.56	0.88	7.74	6.98	10.01
4-5V	52.35	378.90	0.64	5.87	8.78	64.92	263.57	0.87	7.74	6.98	10.13
5-5V	52.06	374.40	0.65	5.94	8.63	64.91	256.73	0.89	7.89	6.87	9.94
1-10V	105.23	770.22	0.64	5.81	8.63	128.73	520.39	0.88	7.81	6.82	10.00
2-10V	103.65	760.63	0.64	5.86	8.70	126.31	510.29	0.89	7.92	6.77	10.04
3-10V	106.18	769.73	0.65	5.80	8.57	129.69	527.12	0.89	7.73	6.83	10.01
4-10V	103.79	762.90	0.64	5.86	8.68	127.52	512.82	0.89	7.89	6.79	10.03
5-10V	104.93	760.64	0.65	5.87	8.58	127.59	522.20	0.89	7.79	6.81	9.98
1-15V	155.09	1136.49	0.64	5.88	8.71	191.43	768.73	0.88	7.90	6.83	10.08
2-15V	157.72	1134.90	0.65	5.89	8.61	191.80	779.56	0.89	7.82	6.83	10.05
3-15V	158.66	1146.47	0.65	5.84	8.59	194.57	782.86	0.89	7.79	6.84	10.01
4-15V	157.00	1133.01	0.65	5.89	8.54	192.36	775.43	0.89	7.85	6.89	10.08
5-15V	157.38	1130.77	0.65	5.89	8.55	192.15	778.34	0.89	7.79	6.83	10.06

One approach to mitigate calendar life losses resulting from non-increasing battery wear function may be to optimize the charging schedule in two phases: first by minimizing energy and degradation costs, and then by minimizing the sum of the periodic SOC variables while constraining total energy and degradation costs to remain below (or within a maximum violation of) the values found in the first phase. This should encourage the model to avoid keeping the batteries in high SOC values for lengthy periods when this can be avoided. We test this idea with the solutions reported in Table 16 by minimizing the sum of the periodic SOC variables while ensuring the same degradation costs and a maximum increase in energy costs of 25%. Table 17 reports the obtained results. The calendar life can indeed be improved, but to ensure the same cycling degradation costs, the battery must still remain above 50% almost at all times, so the calendar aging improvement is limited in this case.

Nevertheless, the same approach can be used with any wear function in order to deal with the time aspect of calendar aging that is not a factor when solely considering cycle aging. For example, charging as closely as possible to departure times is preferable from a calendar aging perspective, but makes no difference from a cycle aging perspective. Such an approach to mitigate calendar aging should, however, include the consideration of FRD charges, since encouraging the charging of vehicles as closely as possible to departure times would most likely require several vehicles being charged simultaneously if routes are clustered during specific portions of the day. The spreading out of routes over the course of the day would thus probably become crucial to keep both calendar aging and FRD charges as low as possible.

Table 17: Costs and average battery life after mitigating calendar aging

Instance	Energy costs	Deg. costs	Avg. Cyc. Life	Avg. Cal. Life
1-5V	75.56	263.75	7.73	7.39
2-5V	72.18	253.72	7.95	7.36
3-5V	73.08	263.56	7.74	7.45
4-5V	73.21	263.57	7.74	7.36
5-5V	73.64	256.73	7.89	7.32
1-10V	148.89	520.39	7.81	7.38
2-10V	146.16	510.29	7.92	7.31
3-10V	149.50	527.12	7.73	7.35
4-10V	147.89	512.82	7.89	7.34
5-10V	147.80	522.20	7.79	7.36
1-15V	219.86	768.73	7.90	7.36
2-15V	221.99	779.56	7.82	7.37
3-15V	223.04	782.86	7.79	7.35
4-15V	220.49	775.43	7.85	7.37
5-15V	220.39	778.34	7.79	7.36

5.5 Precise charging schedules: continuous time model

Although the resolution of the instances with the continuous time model does not provide any new managerial insights, we nevertheless report the continuous time model results for the day and night route instances assuming a constant energy cost equal to the summer mid-peak rate of plan TOU-EV-4 and the degradation costs from Table 2. The results are reported in Table 18.

The continuous time model may come in handy in operational contexts requiring tighter charge scheduling than what is possible by working in discrete time. In the presence of time dependent energy costs, constraints (44) could also be modified to force each charging event to occur during specific time intervals between each consecutive route to ensure taking advantage of lower energy costs during certain periods of the day.

Table 18: Energy and degradation costs for instances with day-time and night-time routes solved with the continuous time model

Instance	Energy costs	Deg. costs	Avg. SOC
1-5V	171.17	1090.90	0.72
2-5V	182.02	1185.98	0.76
3-5V	184.51	1201.30	0.77
4-5V	159.07	998.19	0.68
5-5V	171.26	1093.38	0.72
1-10V	344.83	2206.27	0.73
2-10V	348.10	2243.39	0.74
3-10V	327.36	2064.90	0.69
4-10V	338.30	2153.91	0.71
5-10V	345.22	2217.14	0.73
1-15V	502.56	3206.38	0.72
2-15V	533.09	3447.70	0.75
3-15V	522.91	3365.35	0.74
4-15V	508.42	3251.12	0.72
5-15V	525.60	3393.34	0.74

5.6 The impact of charger related costs

Our numerical experiments with the TOU-EV-4 plan have until now always used the charging infrastructures calibrated in Section 5.1.1 with the instances involving day and night routes in which each route consumes a SOC between 0.45 and 0.9. While such infrastructures allow benefiting from otherwise unachievable energy costs when solving the instances with two shorter routes (i.e., consuming a SOC between 0.40 and 0.47), they are surely not required from a feasibility perspective for these instances. Moreover, the instances with two shorter routes are easier to solve when simultaneously optimizing the charging infrastructure. Therefore, in order to draw some insights regarding the impacts of fixed costs associated with the charging infrastructure, we solved the instances with two short delivery routes (further apart from each other and declustered) while simultaneously optimizing the charging infrastructure with the methodology described in Section 5.1.1. For the scenario in which energy, degradation, charging infrastructure, and FRD costs are all considered simultaneously, the objective function becomes

$$\text{minimize} \quad \sum_{k\in K}\sum_{p\in P}\frac{i_{pk}\cdot\delta}{Q}\cdot QE\cdot c_p+\sum_{r\in R}\sum_{d\in D}QE\cdot\Delta soc_{dr}\cdot W_d+F\cdot c_{FRD}+\sum_{s\in S\setminus\{1\}}C_s\cdot\kappa_s. \quad (72)$$

The results are reported in Table 19 for the summer rates of the TOU-EV-4 plan under several scenarios. The non-decreasing battery wear costs from Table 2 are used whenever degradation costs are jointly minimized. For eight of the experiments, the best found solution had an optimality gap above 0.5% after the five hour time limit, with an optimality gap of 1.79% in the worst case. When nothing is reported in the column indicating the obtained charging infrastructure, no chargers beside the slow level 1 chargers are used in the best found solution.

Table 19: The impact of charger related costs on charging infrastructures and other costs

	Energy, FRD and inf. optimized			Energy, deg., FRD and inf. optimized			Energy and inf. optimized			Energy, deg. and inf. optimized		
Instance	Energy costs	Deg. costs	Inf.	Energy costs	Deg. costs	Inf.	Energy costs	Deg. costs	Inf.	Energy costs	Deg. costs	Inf.
1-5V	69.23	411.50	-	71.82	369.16	-	38.78	410.13	1XS2	67.54	370.75	-
2-5V	60.24	390.78	-	63.19	347.56	-	33.38	390.43	1XS2	58.58	350.31	-
3-5V	68.32	405.87	-	71.42	364.55	-	37.37	424.92	1XS2	67.26	365.66	-
4-5V	69.32	417.50	-	70.52	369.71	-	37.56	422.33	1XS2	67.53	369.80	-
5-5V	64.22	397.31	-	67.29	357.87	-	35.79	401.77	1XS2	62.90	360.53	-
1-10V	101.83	832.59	1XS2	120.89	729.73	1XS2	67.76	824.97	1XS3	85.15	738.57	1XS3
2-10V	95.97	809.56	1XS2	132.92	708.21	-	82.90	794.89	1XS2	121.71	709.41	-
3-10V	96.51	832.81	1XS2	121.95	731.90	1XS2	67.58	831.96	1XS3	81.91	740.67	1XS3
4-10V	97.83	822.43	1XS2	117.84	713.31	1XS2	84.41	803.94	1XS2	83.48	719.22	1XS3
5-10V	100.33	819.53	1XS2	131.40	715.04	-	64.70	805.71	1XS3	121.06	721.76	-
1-15V	159.85	1214.38	1XS2	189.49	1069.55	1XS2	110.19	1189.57	1XS3	136.40	1084.71	1XS3
2-15V	159.47	1240.35	1XS2	190.87	1087.11	1XS2	110.34	1198.53	1XS3	135.87	1102.68	1XS3
3-15V	135.53	1232.85	1XS3	194.71	1092.10	1XS2	113.05	1221.10	1XS3	146.92	1103.36	1XS3
4-15V	157.06	1220.96	1XS2	187.03	1075.10	1XS2	109.17	1191.78	1XS3	137.10	1086.26	1XS3
5-15V	163.31	1229.12	1XS2	191.95	1072.22	1XS2	111.37	1195.06	1XS3	138.78	1090.60	1XS3

As expected, the best found charging infrastructures for these instances are smaller than those obtained in Section 5.1.1. The savings in energy costs obtained by using the faster infrastructures from Section 5.1.1 therefore do not justify the purchase and installation costs of the associated charging equipment for these instances. The results also show that the inclusion of FRD charges when simultaneously optimizing the charging infrastructure usually results in less or slower chargers purchased. Indeed, in order to keep such charges low, the model chooses chargers that consume less power from the grid and is forced to perform more charging during periods of the day with higher electricity rates, thereby demonstrating the trade-off that exists between charging equipment, energy and FRD costs.

The impact of degradation costs on the obtained infrastructures also deserves some comments. If the operational context does not allow much time for inter-route charging, one would expect the inclusion of degradation costs to often result in larger or faster charging infrastructures in order to gain more leeway regarding within which SOC intervals the batteries are cycled and when the bulk of inter-route charging takes place. This is observed when comparing some of the obtained charging infrastructures from Tables 3 and 4 for the instances with long day and night routes. However, when there is ample time for inter-route charging, this is rarely the case. Indeed, the figures from Table 19 show that the best found charging infrastructures almost never become larger or faster when solving a same instance with degradation costs compared to without degradation costs. Finally, it is interesting to note that in a few results from Tables 3, 4 and 19, the obtained charging infrastructure even becomes smaller or slower when solving a same instance with degradation costs compared to without them. This suggests that in some cases, the increase in energy costs that is required in order to always cycle the battery in specific SOC intervals when considering degradation costs no longer justifies the purchase of chargers used to keep energy costs low when solving the problem without degradation costs.

6. Conclusions

The goal of this study was to provide an optimization tool for depot charge scheduling that would integrate several useful considerations, as well as to derive managerial insights through numerical experiments. The model uses realistic charging functions in both discrete and continuous time, with the former also capable of dealing with time-dependent energy costs, grid restrictions and FRD charges. We have also provided tractable methods for integrating an existing battery degradation model into the problem that may be handled by commerical solvers. The tool we have developed can therefore be used to help the business case of EFVs operated in high use rate contexts by mitigating battery degradation occuring at a faster rate as a result of higher vehicle utilization.

Our numerical experiments suggest that degradation costs can be significantly mitigated by incurring slightly higher energy costs. We have also shown that the sum of energy and degradation costs can be controlled more precisely by splitting long routes into shorter ones with respect to SOC consumption, and spreading the routes out over the course of the day. This modification allows more leeway regarding within which SOC intervals the battery is cycled, and during which periods of the day inter-route charging is performed. This may be of interest in operational contexts within which delivery routes stay relatively close to the depot so that vehicles can return to the depot more frequently, and within which vehicles may be allowed perform evening or night-time deliveries. Both of these operational characteristics are more likely to be present in the context of goods distribution with electric vehicles due to their limited range and silent operations.

We have also shown that ignoring FRD charges that may be present in certain electric vehicle charging rate plans for businesses can lead to additional fees that do not justify the associated energy cost savings, but that incurring such fees may be worthwhile in order to keep degradation costs low. Our results also suggest that both FRD charges and degradation costs should be considered when making decisions regarding the depot charging infrastructure. Moreover, we have demonstrated how the model may be used to compare different plans offering tradeoffs between energy costs and FRD charges, and we have illustrated that the presence of grid restrictions may significantly increase energy costs in certain contexts.

We have also concluded that depending on the nature of the cycling wear function (i.e., depending on battery), the integration of calendar aging considerations becomes more or less important. If the cycling wear cost function increases with SOC, then even without calendar aging mitigation, the joint optimization of energy and degradation costs is beneficial to both the cycle and calendar lifetime of the batteries. However, if the cycling wear cost function decreases with SOC, our results suggest that additional steps may be required to mitigate calendar aging in order to avoid spending lengthy periods of time at high SOC values. We have therefore provided a simple methodology to mitigate calendar aging in such scenarios.

Finally, we believe that interesting research avenues lie in the integration of some of the methods discussed in this paper into other problem settings. These may include simultaneously optimizing the charging schedule and assigning vehicles to routes, or even simultaneously routing the vehicles, both of which would require the development of heuristics. Moreover, the proposed methodology for incorporating cycling wear costs is applicable to any electric vehicle routing problem with en route partial recharging, and could thus be used in the future to investigate the impact of such wear costs on solutions of these problems, e.g., it may cause more frequent stops at charging stations in order to cycle the batteries in the SOC intervals with the lowest wear costs.

Acknowledgments

This research was partly supported by the Canadian Natural Sciences and Engineering Research Council under grants 463834-2014, 436014-2013 and 2015-06189. This support is gratefully acknowledged.

Appendix A. Glossary of abbreviations

ACC-DOD: Achievable cycle count as a function of DOD.

CC-CV: Constant current-constant voltage.

DOD: Depth of discharge.

EFV : Electric freight vehicle.

FRD charges: Facilities related demand charges.

SOC: State of charge.

References

Afroditi, A., M. Boile, S. Theofanis, E. Sdoukopoulos, D. Margaritis. 2014. Electric vehicle routing problem with industry constraints: Trends and insights for future research. *Transportation Research Procedia* **3** 452–459.

Barré, A., B. Deguilhem, S. Grolleau, M. Gérard, F. Suard, D. Riu. 2013. A review on lithium-ion battery ageing mechanisms and estimations for automotive applications. *Journal of Power Sources* **241** 680–689.

Bashash, S., S.J. Moura, J.C. Forman, H.K. Fathy. 2011. Plug-in hybrid electric vehicle charge pattern optimization for energy cost and battery longevity. *Journal of Power Sources* **196** 541–549.

Bruglieri, M., F. Pezzella, O. Pisacane, S. Suraci. 2015. A variable neighborhood search branching for the electric vehicle routing problem with time windows. *Electronic Notes in Discrete Mathematics* **47** 221–228.

Conrad, R.G., M.A. Figliozzi. 2011. The recharging vehicle routing problem. In: Doolen, T., Van Aken, E., eds. *Proceedings of the 2011 Industrial Engineering Research Conference*. Reno, Nevada.

Davis, B.A., M.A. Figliozzi. 2013. A methodology to evaluate the competitiveness of electric delivery trucks. *Transportation Research Part E* **49**(1) 8–23.

eMotorWerks. 2017. JuiceBox EV Charging Stations. URL `https://emotorwerks.com/products/juicebox`. Last accessed 6/6/2017.

E-Mobility NSR. 2013. Comparative analysis of european examples of schemes for freight electric vehicles - Compilation report. E-Mobility NSR, Aalborg, Denmark. URL `http://e-mobility-nsr.eu/fileadmin/user_upload/downloads/info-pool/E-Mobility_-_Final_report_7.3.pdf`. Last accessed 15/6/2017.

Felipe, Á., M.T. Ortuño, G. Righini, G. Tirado. 2014. A heuristic approach for the green vehicle routing problem with multiple technologies and partial recharges. *Transportation Research Part E* **71** 111–128.

Feng, W., M. Figliozzi. 2013. An economic and technological analysis of the key factors affecting the competitiveness of electric commercial vehicles: A case study from the USA market. *Transportation Research Part C* **26** 135–145.

Franceschetti, A.,D. Honhon, G. Laporte, T. Van Woensel, J.C. Fransoo. 2017. Strategic fleet planning for city logistics. *Transportation Research Part B* **95** 19–40.

Goeke, D., M. Schneider. 2015. Routing a mixed fleet of electric and conventional vehicles. *European Journal of Operational Research* **245**(1) 81–99.

Han, S., S. Han, H. Aki. 2014. A practical battery wear model for electric vehicle charging applications. *Applied Energy* **113** 1100–1108.

Hiermann, G., J. Puchinger, S. Ropke, R.F. Hartl. 2016. The electric fleet size and mix vehicle routing problem with time windows and recharging stations. *European Journal of Operational Research* **252**(3) 995–1018.

Hoke, A., A. Brissette, D. Maksimović, A. Pratt, I. Labs, K. Smith. 2011. Electric vehicle charge optimization including effects of lithium-ion battery degradation. *2011 IEEE Vehicle Power and Propulsion Conference (VPPC)*. IEEE, Chicago, Illinois, 1–8.

Lam, L. 2011. A practical circuit-based model for state of health estimation of li-on battery cells in electric vehicles. Master's thesis, Delft University of Technology, Delft, The Netherlands.

Lebeau, P., C. De Cauwer, J. Van Mierlo, C. Macharis, W. Verbeke, T. Coosemans. 2015. Conventional, hybrid, or electric vehicles: Which technology for an urban distribution centre? *The Scientific World Journal*, Article ID 302867.

Lee, D.Y., V.M. Thomas, M.A. Brown. 2013. Electric urban delivery trucks: Energy use, greenhouse gas emissions, and cost-effectiveness. *Environmental Science & Technology* **47**(14) 8022–8030.

Lunz, B., Z. Yan, J.B. Gerschler, D.U. Sauer. 2012. Influence of plug-in hybrid electric vehicle charging strategies on charging and battery degradation costs. *Energy Policy* **46** 511–519.

Marra, F., G.Y. Yang, C. Traholt, E. Larsen, C.N. Rasmussen, S. You. 2012. Demand profile study of battery electric vehicle under different charging options. *2012 IEEE Power and Energy Society General Meeting*. IEEE, San Diego, California, 1–7.

Montoya, A., C. Guéret, J.E. Mendoza, J.G. Villegas. 2017. The electric vehicle routing problem with nonlinear charging function. *Transportation Research Part B*, https://doi.org/10.1016/j.trb.2017.02.004.

Naberezhnykh, D., J J. Wardle, J J. Lowes, C. Herron, T. Brightman, T. Parker. 2012. Electric vehicle charging points for freight vehicles in central London. Prepared for Central London FQP by Transport & Travel Research Ltd, in partnership with TRL and Zero Carbon Futures. URL `http://www.centrallondonfqp.org/app/download/12240926/CLFQP_EVCP_strategy+report_Final+v1+0.pdf`. Last accessed 15/6/2017.

Nesterova, N., H. Quak, S. Balm, I. Roche-Cerasi, T. Tretvik. 2013. Project FREVUE deliverable D1.3: State of the art of the electric freight vehicles implementation in city logistics. TNO and SINTEF. European Commission Seventh Framework Programme.

Pelletier, S., O. Jabali, G. Laporte. 2016. 50th Anniversary Invited Article - Goods Distribution with Electric Vehicles: Review and Research Perspectives. *Transportation Science* **50**(1) 3–22.

Pelletier, S., O. Jabali, G. Laporte, M. Veneroni. 2017. Battery degradation and behaviour for electric vehicles: Review and numerical analyses of several models. *Transportation Research Part B*, https://doi.org/10.1016/j.trb.2017.01.020.

Preis, H., S. Frank, K. Nachtigall. 2014. Energy-optimized routing of electric vehicles in urban delivery systems. In: Helber, S., Breitner, M., Rösch, D., Schön, C. Graf von der Schulenburg, J-M., Sibbertsen, P., Steinbach, M., Weber, S., Wolter, A., eds. *Operations Research Proceedings 2012*. Springer International Publishing, Heidelberg, 583–588.

Quak, H., N. Nesterova, T. van Rooijen. 2016. Possibilities and barriers for using electric-powered vehicles in city logistics practice. *Transportation Research Procedia* **12** 157–169.

Sassi, O., A. Oulamara. 2014a. Joint Scheduling and Optimal Charging of Electric Vehicles Problem. In: Murgante, B., et al. (eds.)) ICCSA 2014, Part II. LNCS, vol. 8580, pp. 7691. Springer, Heidelberg (2014).

Sassi, O., A. Oulamara. 2014b. Simultaneous Electric Vehicles Scheduling and Optimal Charging in the Business Context: Case Study. 5th IET Hybrid and Electric Vehicles Conference (HEVC 2014), London, 2014, pp. 1–6. doi: 10.1049/cp.2014.0954

Schiffer, M., G. Walther. 2015. The electric location routing problem with time windows and partial recharging. Working paper OM-01/2015, Chair of Operations Management, RWTH

Aachen University. URL http://www.om.rwth-aachen.de/data/uploads/om-012015.pdf. Last accessed 14/6/2016.

Schiffer, M., G. Walther. 2016. An adaptive large neighborhood search for the location routing problem with intraroute facilities. Working paper OM-01/2016, Chair of Operations Management, RWTH Aachen University. URL http://www.om.rwth-aachen.de/data/uploads/om-012016.pdf. Last accessed 14/6/2016.

Schneider, M., A. Stenger, D. Goeke. 2014. The electric vehicle-routing problem with time windows and recharging stations. *Transportation Science* **48**(4) 500–520.

Taefi, T.T. 2016. Viability of electric vehicles in combined day and night delivery: a total cost of ownership example in Germany. *European Journal of Transport and Infrastructure Research* **16**(4) 600–618.

Taefi, T.T., S. Stütz, A. Fink. 2016. Increasing the mileage of battery electric medium duty vehicles: A recipe for competitiveness? Helmut-Schmidt-University Hamburg, Institute of Computer Science Research Paper Series, Research Paper 16–01.

Tremblay, O., L.-A. Dessaint, A.-I. Dekkiche. 2007. A generic battery model for the dynamic simulation of hybrid electric vehicles. *2007 Vehicle Power and Propulsion Conference*. IEEE, Arlington, Texas, 284–289.

Soutern California Edison. 2017. Electric Car Rate Options. URL sce.com/wps/portal/home/business/rates/electric-car-business-rates. Last accessed 6/6/2017.

Yang, J., H. Sun. 2015. Battery swap station location-routing problem with capacitated electric vehicles. *Computers & Operations Research* **28** 217–232.